

U.S. DEPARTMENT OF COMMERCE  
National Technical Information Service

AD-A033 647

STUDIES OF HOMOGENEOUS AND HETEROGENEOUS HYDRAZINE  
DECOMPOSITION FOR MONOPROPELLANT PROPULSION SYSTEMS

STANFORD RESEARCH INSTITUTE, MENLO PARK, CALIFORNIA

SEPTEMBER 1976

AFOSR - TR - 76 - 1412  
364116

September 1976

Annual Report  
Covering the Period June 1, 1975-May 31, 1976

STUDIES OF HOMOGENEOUS AND HETEROGENEOUS HYDRAZINE  
DECOMPOSITION FOR MONOPROPELLANT PROPULSION SYSTEMS

By: D. Golden, K. E. Lewis, R. T. Rewick, S. E. Stein, and H. Wi:

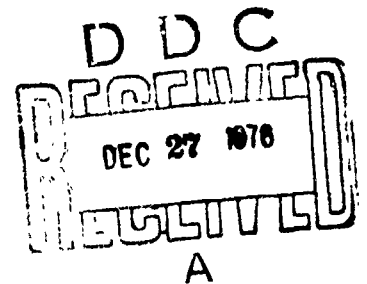
Prepared for:

AIR FORCE OFFICE OF SCIENTIFIC RESEARCH  
1400 Wilson Boulevard  
Arlington, Virginia 22209

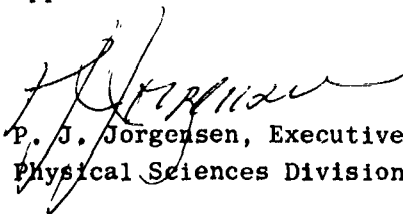
Attention: Thomas C. Meier, Major, USAF  
Program Manager  
Directorate of Aerospace Sciences

AFOSR Contract F44620-73-C-0069

SRI Project PYU-2716



Approved:

  
P. J. Jorgensen, Executive Director  
Physical Sciences Division



STANFORD RESEARCH INSTITUTE  
Menlo Park, California 94025 · U.S.A.

REPRODUCED BY  
NATIONAL TECHNICAL  
INFORMATION SERVICE  
U. S. DEPARTMENT OF COMMERCE  
SPRINGFIELD, VA. 22161

DISTRIBUTION STATEMENT A  
Approved for public release;  
Distribution Unlimited

REPORT DOCUMENTATION PAGE		READ INSTRUCTIONS BEFORE COMPLETING FORM
1. REPORT NUMBER <b>AFOSR - TR - 76 - 1412</b>	2. GOVT ACCESSION NO.	3. RECIPIENT'S CATALOG NUMBER
4. TITLE (and Subtitle)  <b>STUDIES OF HOMOGENEOUS AND HETEROGENEOUS HYDRAZINE DECOMPOSITION FOR MONOPROPELLANT PROPULSION SYSTEMS</b>		5. TYPE OF REPORT & PERIOD COVERED <b>INTERIM</b> <b>1 June 1975 - 31 May 1976</b>
		6. PERFORMING ORG. REPORT NUMBER
7. AUTHOR(s) <b>D GOLDEN                    S E STEIN K E LEWIS                 H WISE R T REWICK</b>		8. CONTRACT OR GRANT NUMBER(s)  <b>F44620-73-C-0069</b>
9. PERFORMING ORGANIZATION NAME AND ADDRESS <b>STANFORD RESEARCH INSTITUTE MENLO PARK, CALIFORNIA 94025</b>		10. PROGRAM ELEMENT, PROJECT, TASK AREA & WORK UNIT NUMBERS <b>681308 2308A1 61102F</b>
11. CONTROLLING OFFICE NAME AND ADDRESS <b>AIR FORCE OFFICE OF SCIENTIFIC RESEARCH/NA BLDG 410 BOLLING AIR FORCE BASE, D C 20332</b>		12. REPORT DATE <b>Sep 76</b>
		13. NUMBER OF PAGES <b>48-                    50</b>
14. MONITORING AGENCY NAME & ADDRESS (if different from Controlling Office)		15. SECURITY CLASS. (of this report)  <b>UNCLASSIFIED</b>
		15a. DECLASSIFICATION/DOWNGRADING SCHEDULE
16. DISTRIBUTION STATEMENT (of this Report)  <b>Approved for public release; distribution unlimited.</b>		
17. DISTRIBUTION STATEMENT (of the abstract entered in Block 20, if different from Report)		
18. SUPPLEMENTARY NOTES		
19. KEY WORDS (Continue on reverse side if necessary and identify by block number) <b>HYDRAZINE MONOPROPELLANTS SPACE PROPULSION</b>		
20. ABSTRACT (Continue on reverse side if necessary and identify by block number) <b>Heterogeneous kinetic studies of hydrazine decomposition at atmospheric and subatmospheric pressures and infrared absorption measurements on alumina- supported iridium catalysts point to a reaction intermediate as the surface contaminant responsible for catalyst deactivation. The temperature region around 450 K has been found to be most detrimental to catalyst life under laboratory test conditions for hydrazine decomposition.</b>		

## CONTENT

I	INTRODUCTION . . . . .	1
II	EXPERIMENTAL DETAILS . . . . .	3
	A. Atmospheric Pressure Reactor . . . . .	3
	B. Low Pressure Reactor . . . . .	3
	C. Infrared Studies . . . . .	6
	1. Description of Apparatus . . . . .	6
	2. Catalyst Preparation . . . . .	7
III	RESULTS . . . . .	
	A. High-Pressure Studies . . . . .	8
	B. Low-Pressure Studies . . . . .	8
	C. Infrared Studies . . . . .	11
IV	DISCUSSION . . . . .	14
V	CONCLUSION . . . . .	19
VI	REFERENCES . . . . .	20

## ILLUSTRATIONS

1.	Knudsen Flow Reactor (R1) for Measuring Rate of $N_2H_4$ Decomposition on Shell-405 Catalyst . . . . .	27
2.	Fused Silica Dual-Chamber Low Pressure Flow Reactor (R2) . . . . .	28
3.	Schematic Diagram of Differentially Pumped Modulated Molecular Beam Mass Spectrometric Detection System for Low Pressure Flow Reactor. . . . .	29
4.	The Infrared Cell . . . . .	30

**Preceding page blank**

5.	Catalyst Activity Decrease as a Function of Temperature and $N_2H_4$ Exposure . . . . .	31
6.	Catalyst Activity Decrease After Exposure to $8.0 \times 10^3$ mole $N_2H_4$ (10 wt% Ir/ $Al_2O_3$ ) . . . . .	32
7.	Effect of Catalyst Particle Size on Activity Decline at 298 K . . . . .	33
8.	Arrhenius Plot of High-Temperature $N_2H_4$ Decomposition on Shell-405 . . . . .	34
9.	Reactivity of Activated Shell-405 for $N_2H_4$ Decomposition . . . . .	35
10.	Measure of $N_2H_4$ Decomposition as a Function of Flow Rate. . . . .	36
11.	Decomposition of Ammonia on Fresh Shell-405 (32 wt% Ir) . . . . .	37
12.	Comparison of $N_2H_4$ and $NH_3$ Reaction Probability on Two Samples of Fresh Shell-405 . . . . .	38
13.	Reversible Deactivation of Shell-405 Catalyst Resulting from $N_2H_4$ Exposure at 298 K . . . . .	39
14.	Effect of $N_2H_4$ Exposure on Delay Time . . . . .	40
15.	Catalyst Deactivation by CO Exposure at 298 K . . . . .	41
16.	Infrared Spectrum of Ir/ $Al_2O_3$ Exposed to $N_2H_4$ ( $6.0 \times 10^{-3}$ moles) . . . . .	42
17.	Formation of 3335, 1603, and $1499\text{ cm}^{-1}$ Bands on Ir/ $Al_2O_3$ as a Function of $N_2H_4$ Exposure . . . . .	43
18.	Kinetic Analysis of Formation Rates of 3335, 1603, and $1499\text{ cm}^{-1}$ Bands on Ir/ $Al_2O_3$ as a Function of $N_2H_4$ Exposure . . . . .	44
19.	Effect of $H_2$ on Catalyst Deactivation During $N_2H_4$ Exposure at 373 K . . . . .	45

TABLES

1.	Reactivation of Ir/Al <sub>2</sub> O <sub>3</sub> Catalyst in He at Various Temperatures . . . . .	21
2.	Summary of IR Spectra Observed on Ir/Al <sub>2</sub> O <sub>3</sub> and on Al <sub>2</sub> O <sub>3</sub> Exposed to N <sub>2</sub> H <sub>4</sub> or NH <sub>3</sub> . . . . .	22
3.	Specific Surface Assignments for Infrared Bands Found on N <sub>2</sub> H <sub>4</sub> -Exposed Ir/Al <sub>2</sub> O <sub>3</sub> . . . . .	23
4.	Effect of N <sub>2</sub> H <sub>4</sub> Exposure on Infrared Bands Observed on Ir/Al <sub>2</sub> O <sub>3</sub> . . . . .	24
5.	Effect of Heating in He on Absorption Spectrum of Ir/Al <sub>2</sub> O <sub>3</sub> Exposed to Hydrazine . . . . .	25
6.	Effect of H <sub>2</sub> on the Infrared Spectrum of N <sub>2</sub> H <sub>4</sub> -Exposed Ir/Al <sub>2</sub> O <sub>3</sub> . . . . .	26

REPRODUCED  
 REPRODUCED  
 REPRODUCED  
 BY \_\_\_\_\_  
 FOR \_\_\_\_\_  
 DATE \_\_\_\_\_  
 FILE NO. \_\_\_\_\_  
 SEC. \_\_\_\_\_  
 A

## I INTRODUCTION

For several years, considerable effort has been devoted to developing a  $N_2H_4$  fueled monopropellant control thruster capable of reliable and prolonged operation in a space environment. Current monopropellant engines use a Shell-405 catalyst bed (an alumina-supported iridium catalyst) to decompose liquid hydrazine into hot gaseous products. However, during repetitive operation of such engines in a limited pulse mode cycle, the catalytic reactor exhibits a gradual loss of thrust generally attributed to a deterioration in catalyst performance. Ultimately "washout" occurs, a process in which liquid  $N_2H_4$  penetrates through the catalyst bed without decomposition.

The mechanisms by which loss in catalyst activity are thought to occur can generally be separated into two categories:

- The physical breakup of the catalyst caused by either thermal shocks over the large temperature range experienced during operation, or large pressure gradients generated within the catalyst particle resulting from pore wetting by liquid reactant.
- Catalyst poisoning, i.e., the adsorption of surface species on a significant part of the catalyst surface.

Earlier studies of the mechanism of hydrazine decomposition on evaporated film of tungsten and molybdenum<sup>1,2</sup> have indicated that N-H and N-N bonds break during the catalytic decomposition of  $N_2H_4$ , with different mechanisms and products prevailing at high and low temperatures. Our studies with polycrystalline Ir<sup>3</sup> and alumina-supported Ir crystallites<sup>4</sup> (Shell-405) have identified the presence of hydrogen and nitrogen adatoms

with several distinct binding states on the surface of the metal. Our results suggest that strongly bound nitrogen adspecies formed during  $N_2H_4$  decomposition can contribute to the loss of catalyst activity encountered during  $H_2H_4$  exposure.

During the current program year, we have studied in detail the mechanism of surface adsorbate formation, with the objectives of: (1) relating catalyst activity decline to  $N_2H_4$  exposure at different temperatures, (2) determining  $N_2H_4$  and  $NH_3$  decomposition kinetics at low pressures in the absence of concentration and temperature gradients in the reactor, and (3) identifying by infrared absorption studies the surface intermediates responsible for catalyst deactivation.

Section II describes our experimental approach to these studies, in Sections III and IV we present and discuss our results. Our conclusions are set forth in Section V.

## II EXPERIMENTAL DETAILS

### A. Atmospheric Pressure Reactor

A powdered sample of catalyst ( $5.5 \times 10^{-3}$  g of 10 wt% Ir/Al<sub>2</sub>O<sub>3</sub>), was placed in a differential flow reactor and exposed to a stream of gaseous hydrazine. The reactant stream ( $\sim 2$  vol% N<sub>2</sub>H<sub>4</sub>, 98 vol% He) was generated by bubbling He through liquid N<sub>2</sub>H<sub>4</sub> (Olin Technical Grade) at room temperature, followed by additional He dilution. After a specified length of exposure at elevated temperatures, the catalyst was examined for activity by passing over it a pulse of N<sub>2</sub>H<sub>4</sub> vapor ( $6.3 \times 10^{-6}$  moles) in a He carrier stream at 300 K. The degree of N<sub>2</sub>H<sub>4</sub> conversion was determined by gas chromatographic analysis of the mass of N<sub>2</sub> formed. This measurement accurately describes catalyst activity, since only NH<sub>3</sub> and N<sub>2</sub> are products of the decomposition at 300 K. Before admission of the sample to the gas chromatograph, we removed NH<sub>3</sub> and unreacted N<sub>2</sub>H<sub>4</sub> from the product stream by condensation in a cold trap (cooled by liquid nitrogen) to avoid interference with the N<sub>2</sub> measurement.

### B. Low Pressure Reactor

Two fused-silica reactors were used. Both were operated under Knudsen flow conditions where the mean-free path of the reactant molecules is greater than the diameter of the catalyst pellet and the reactor exit aperture. The first reactor (R1, Figure 1) was a cylindrical quartz chamber into which several catalyst pellets of Shell-405 were placed. A gas mixture composed of gaseous hydrazine and inert gas (argon) enters the reactor. A mass spectrometer is used to

continually sample the product mixture flowing through the exit aperture. The fractional decomposition of reactant is determined by comparing mass spectral signals of product to reactant and inert gas. Reactor R1 was used for most of the studies with the exception of the measurements of low-temperature catalyst deactivation by  $N_2H_4$  ( $300\text{ K} < T \lesssim 550\text{ K}$ ), for which Reactor R2 (Figure 2) was used.

Reactor R2 consists of two chambers separated by a valve. The gas flows into a quartz chamber with an exit aperture. The gas flow can be directed to a neighboring, catalyst-containing chamber by operating the externally activated valve. Since the conductance of the open valve is much larger than that of the exit aperture, the two chambers are effectively unified. The fractional disappearance of reactant may be directly measured by monitoring reactants with the valve open and closed, thereby exposing and bypassing the catalyst. The relative conversion of reactant may thus be determined without reference to a calibration signal for the inert carrier gas. For analysis, the gases exiting from the reactor are formed into a molecular beam, which is chopped with a rotating chopping wheel and mass spectrometrically detected by use of phase-sensitive electronics. This detection system (Figure 3) ensures that the gas mixture flowing from the reactor is monitored before adsorption and reaction downstream of the reactor.

The technique is termed very low pressure pyrolysis (VLPP) and is fully described in Reference 5. If a species, B, can react by a first-order reaction or effuse from the reactor, we have the simple pseudo-chemical system:



Under Knudsen conditions (stirred flow-reactor), we have

$$k_e = \frac{\bar{C} A_e}{4V} \quad ; \text{ where } \bar{C} \text{ is the mean velocity,}$$

$A_e$  is the aperture area, and  
 $V$  is the volume of the reactor.

$$k_d = P_c k_c = \frac{P_c \bar{C} A_c}{4V} \quad ; \text{ where } P_c \text{ is the reaction probability}$$

per collision with the external  
 surface of the catalyst  $A_c$

The rate constants  $k_e$  and  $k_d$  refer to Equations (1) and (2).

In the absence of catalytic reaction the average concentration of reactant in the reactor is given by:

$$(B)_o = F_B / k_e V, \text{ where } F_B \text{ is the flux of B into the reactor.}$$

In the presence of catalyst,

$$(B) = \frac{F_B}{(k_e + k_d) V} \quad ,$$

Thus,

$$\frac{(B)_o}{(B)} = \frac{k_e + k_d}{k_e} = 1 + \frac{k_d}{k_e} \quad ,$$

and

$$\frac{(B)_o - (B)}{(B)} = \frac{k_d}{k_e} = \frac{P_c k_c}{k_e} = P_c \frac{A_c}{A_e} \quad .$$

Therefore,

$$P_c = \frac{A_e}{A_c} \frac{(B)_o - (B)}{(B)} \quad (3)$$

If we define the fraction decomposed as

$$f_d \equiv \frac{(B)_o - (B)}{(B)_o}$$

then,

$$P_c = \frac{A_e}{A_c} \left( \frac{f_d}{1 - f_d} \right) \quad (4)$$

It can be shown that if  $P_c$  is independent of  $F_B$ , the process is first-order. Otherwise, its order dependence must be determined. For Knudsen flow in our apparatus, the gas pressures used are in the  $10^{-3}$  torr range.

### C. Infrared Studies

#### 1. Description of Apparatus

The 10-cm Pyrex infrared cell used for this study is "T" shaped<sup>6</sup> as shown in Figure 4. The outside of the vertical section is wrapped with resistance wire and provided with a thermowell for temperature measurement. The end plates of the horizontal section of the cell are equipped with NaCl windows. The catalyst is deposited on a  $BaF_2$  crystal which can be raised and lowered into the vertical section of the cell by means of a specially designed Teflon stopcock provided with a Pyrex string attached to the crystal. For ir measurements the crystal is lowered into the horizontal window section before and after exposure to gases at elevated temperatures or during exposure to gaseous reactants or inert carrier gas (He or Ar) at room temperature. Infrared spectra are obtained during flow conditions at 1 atmosphere total pressure with a Perkin-Elmer Model 457 spectrometer. With the catalyst samples under study, good spectral transmission was achieved in the frequency region 4000 to  $1200\text{ cm}^{-1}$ . A scan over this spectral region is sufficient to detect most of the reported OH and NH vibrational frequencies. Hydrazine

is vaporized by bubbling He at a slow rate through a liquid sample to give a saturated vapor stream ( $\sim 2$  vol%), which is subsequently diluted with additional He to  $\sim 1$  vol% before it enters the cell.

## 2. Catalyst Preparation

The catalyst is prepared by depositing five  $0.05 \text{ cm}^3$  aliquots of an aqueous dispersion of  $\text{IrCl}_4$  in colloidal  $\text{Al}_2\text{O}_3$  (Baymal) on each side of the  $\text{BaF}_2$  crystal ( $8 \times 8 \times 25$  mm). Each aliquot is spread to wet the entire optical surfaces and is then evaporated to dryness with an ir heat lamp before the next aliquot is added. By this technique, 3 mg of  $\sim 10$  wt% Ir on  $\text{Al}_2\text{O}_3$  can be dispersed. This technique was also used to prepare a blank containing only  $\text{Al}_2\text{O}_3$ . Before study, the catalyst was reduced in  $\text{H}_2$  at 723 K for 30 min, flushed in He at 723 K for 10 min, then cooled to room temperature.

### III RESULTS

#### A. High-Pressure Studies

A gradual decay in catalytic conversion of  $N_2H_4$  was detected for an Ir/ $Al_2O_3$  catalyst sample exposed to  $N_2H_4$  in a He carrier stream at various temperatures, and subsequently examined for activity in a pulse mode at 300 K. The rate of decay appeared to be a sensitive function of catalyst temperature (Figure 5). The highest degree of catalyst deactivation occurred near 450 K (Figure 6). This deactivation could be partially reversed by heating the catalyst in a He carrier stream. However, temperatures above 673 K were required to approach the initial level of activity (Table 1), indicating that a strongly bound adspecies may be the cause of catalyst poisoning under our experimental conditions.

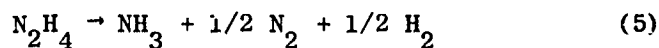
To determine the influence of the pore structure of Shell-405 catalyst in  $N_2H_4$  decomposition, we compared the loss in catalytic activity of pelletized and powdered samples (Figure 7). The pelletized sample exhibited a much more rapid decline in catalytic activity than did the powdered sample. The Ir crystallite within the internal pore structure of the pellet obviously cannot participate to any large extent in the  $N_2H_4$  decomposition reaction.

#### B. Low-Pressure Studies

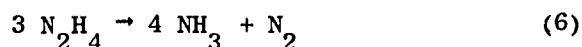
We have found two distinctly different temperature regimes of  $N_2H_4$  decomposition on Ir/ $Al_2O_3$ : in the range above approximately 600 K, a reproducible exposure-independent decomposition is observed; below 550 K, an exposure-dependent decomposition with rather complex kinetics

is noted. Ammonia decomposition to  $N_2$  and  $H_2$  is detectable above approximately 600 K.

The following reaction, independent of the  $N_2H_4$  exposure, was found to prevail at temperatures greater than 600 K (Figure 8):



The activation energy,  $E_{act}$ , was found to be  $2.2 \pm 0.3$  kcal mol<sup>-1</sup>. Below 550 K, ammonia and nitrogen are the only products of  $N_2H_4$  decomposition in accordance with the stoichiometry:



on both active and partially poisoned Ir/Al<sub>2</sub>O<sub>3</sub>. Active catalyst surfaces could be generated by heating to 1000 K in H<sub>2</sub>. The activity was determined before measurable poisoning caused by exposure to  $N_2H_4$  at temperatures below 600 K. As shown by the data in Figure 9, activity reaches a minimum near 425 to 450 K, and its temperature dependence in this region cannot be fitted by a single arrhenius expression. The initial reaction probability is high ( $> 0.1$  collision<sup>-1</sup>); however, because of the strong dependence of activity on exposure to technical grade hydrazine, our study of the initial activity has been limited. Also small pressure dependence was noted for this reaction over the temperature range 298 to 873 K both for fresh and partially poisoned catalyst samples (Figure 10).

The catalytic decomposition of  $NH_3$  to  $N_2$  and  $H_2$  was found to occur on Ir/Al<sub>2</sub>O<sub>3</sub> catalyst above 600 K (Figure 11). On two catalyst samples of somewhat differing activity the rate of  $NH_3$  decomposition was found to be approximately one-tenth the rate for  $N_2H_4$  decomposition (Figure 12). Although more careful analyses of the flow and temperature dependence

of the relative rate of the  $\text{NH}_3$  reaction versus the  $\text{N}_2\text{H}_4$  reaction was needed, the  $\text{NH}_3$  reaction appears to be a convenient, albeit an indirect, probe for activity evaluation of the catalyst.

In agreement with the high-pressure studies discussed in the preceding section, a gradual decay in catalyst activity was noted on exposure to technical grade hydrazine below 600 K. Typical results are shown in Figure 13. Exposing such a poisoned catalyst to a flow of  $\text{H}_2$  at low temperatures, or leaving the catalyst in the reactor for several days does not restore initial activity. However, heating above 700 K completely rejuvenated the catalyst. In addition, the activity of catalyst poisoned at room temperature could be temporarily restored by heating to 400 K (approximately 80% of the initial activity). However prolonged exposure at 400 K resulted in poisoning.

With Reactor R2, we have noted an interesting and potentially important aspect of  $\text{N}_2\text{H}_4$  decomposition on exposure-poisoned  $\text{Ir}/\text{Al}_2\text{O}_3$ . The onset of  $\text{N}_2$  and  $\text{NH}_3$  product appearance follows  $\text{N}_2\text{H}_4$  exposure with a delay time that increases monotonically with exposure poisoning. If this delay,  $\tau_d$  (298 K), is defined as the time interval between  $\text{N}_2\text{H}_4$  exposure at 298 K (valve in R2 is opened to begin exposure to the catalyst) and appearance of products, then for unpoisoned catalyst,  $\tau_d$  (298 K) is approximately 1 to 3 sec, whereas for a catalyst poisoned by  $\text{N}_2\text{H}_4$  exposure to 50% of this initial activity,  $\tau_d$  (298 K) is approximately 15 to 30 sec (Figure 14).

Exposure of  $\text{Ir}/\text{Al}_2\text{O}_3$  pellets to CO at 298 K was found to reduce catalytic activity for  $\text{N}_2\text{H}_4$  decomposition. Figure 15 shows such deactivation for fresh and partially  $\text{N}_2\text{H}_4$ -exposure poisoned catalyst. The initial rapid deactivation may result either from poisoning of the most accessible active sites near the surface or from selective poisoning on specially susceptible reaction sites.

At 800 K, exposure to toluene was found to cause catalyst deterioration. Activity was reduced by roughly one-half after exposure to approximately  $10^{19}$  molecules at this temperature. Additional quantities of toluene had little further effect on activity. In this regard, this poisoning effect is similar to  $N_2H_4$ - and CO-induced deactivation at lower temperature. At 900 K,  $O_2$  exposure was found to completely restore the activity. Most likely, the carbon deposited on the surface by toluene decomposition reacts to form CO which readily desorb at this high temperature.<sup>7</sup>

### C. Infrared Studies

Figure 16 shows a typical infrared spectrum obtained for the Ir/ $Al_2O_3$  catalyst and the  $Al_2O_3$  blank after 16 hours exposure to  $N_2H_4$  ( $\sim 6 \times 10^{-3}$  moles). Although the magnitude of absorption-band intensities can only be evaluated semiquantitatively because small peak-overlap corrections have not been made, the bands observed can be assigned to OH, NH, and  $NH_2$  absorption frequencies in addition to molecularly adsorbed  $N_2H_4$  and  $NH_3$  (Table 2). While many of the absorption bands are common to both the  $Al_2O_3$  support ("blank") and the Ir/ $Al_2O_3$  catalyst, the absorption bands at 1499 and 1469  $cm^{-1}$  are found only on Ir/ $Al_2O_3$ . These absorption bands can be assigned to frequencies characteristic of  $NH_2$  and  $NH_4^+$  species, respectively. Comparison of the spectra observed for Ir/ $Al_2O_3$  exposed to  $N_2H_4$  and to  $NH_3$  indicates that the band at 1499  $cm^{-1}$  is formed only during  $N_2H_4$  exposure, whereas the 1469  $cm^{-1}$  band appears associated with both  $NH_3$  and  $N_2H_4$  (Table 2). Exposures of the  $Al_2O_3$  support to  $N_2H_4$  and  $NH_3$  result in spectra in which the bands at 1499 and 1469  $cm^{-1}$  are absent. The band at 1623  $cm^{-1}$  appears to be characteristic of OH or adsorbed molecular  $N_2H_4$ . From a comparison of data given in Table 2, the ir spectrum of  $N_2H_4$ -exposed Ir/ $Al_2O_3$  can be simplified in terms of specific surface assignments. As shown

in Table 3, the ir bands at  $\sim 3474$ ,  $1623$ , and  $1603 \text{ cm}^{-1}$  are associated with the  $\text{Al}_2\text{O}_3$  surface, and those at  $1499$  and  $1469 \text{ cm}^{-1}$ , with the Ir surface.

All bands, except those at  $\sim 3474 \text{ cm}^{-1}$  (OH) and  $1469 \text{ cm}^{-1}$  ( $\text{NH}_4^+$ ), are observed to increase with  $\text{N}_2\text{H}_4$  exposure (Table 4). The bands showing the largest intensity increase are located at  $1603 \text{ cm}^{-1}$  ( $\text{N}_2\text{H}_4/\text{Al}_2\text{O}_3$ ) and at  $1499 \text{ cm}^{-1}$  ( $\text{NH}_2/\text{Ir}$ ).

Over a range of exposures to  $\text{N}_2\text{H}_4$ , significant changes in peak intensities occur for bands associated with  $\text{N}_2\text{H}_4$ ,  $\text{NH}_3$  ( $3335 \text{ cm}^{-1}$ ),  $\text{N}_2\text{H}_4$  ( $1603 \text{ cm}^{-1}$ ), and  $\text{NH}_2$  ( $1499 \text{ cm}^{-1}$ ) frequencies (Figure 17). From the initial slope of the data shown, we estimate the rate of formation of the  $\text{N}_2\text{H}_4/\text{NH}_3$  band to be about a factor of 2 greater than that for the  $\text{N}_2\text{H}_4$  and  $\text{NH}_2$  bands. Kinetic analysis of the formation of these bands can be made from the typical Langmuir type of first and second order rate laws

$$d\theta/dt = k(1-\theta) \quad (7)$$

and

$$d\theta/dt = k(1-\theta)^2 \quad (8)$$

where  $\theta$  = fractional monolayer coverage

Integration of Equations (7) and (8) between the limits 0 to  $\theta$  provides the expressions

$$kt = -\ln(1-\theta) \quad (9)$$

and

$$kt = \theta/1-\theta \quad (10)$$

Using the data given in Figure 17 to obtain values for  $\theta$ , we find that Equations (9) and (10) can be used to interpret the formation of the 3335, 1603, and 1499  $\text{cm}^{-1}$  bands. The band at 1499  $\text{cm}^{-1}$  ( $\text{NH}_2/\text{Ir}$ ) is found to be of second order in the unoccupied site density,  $s$ , on the metal surface, i.e.,  $\text{N}_2\text{H}_4 + 2s \rightarrow 2 (\text{NH}_2-s)$ . The other two follow first-order kinetics (Figure 18).

The relative binding strengths of the surface adsorbates seen by ir spectroscopy can be deduced from measurements of the change in absorbance as a function of temperature in a He carrier stream. The results (Table 5) indicate that at 373 K, all the band intensities are reduced to near background levels, except those at 1603  $\text{cm}^{-1}$  ( $\text{N}_2\text{H}_4/\text{Al}_2\text{O}_3$ ), 1499  $\text{cm}^{-1}$  ( $\text{NH}_2/\text{Ir}$ ), and 1469  $\text{cm}^{-1}$  ( $\text{NH}_4^+/\text{Ir}$ ). The last two band intensities show the smallest changes over the entire temperature range studied. Exposure of the catalyst to  $\text{N}_2\text{H}_4$  at room temperature yields an absorption spectrum comparable to that seen before heating in He.

When  $\text{Ir}/\text{Al}_2\text{O}_3$  is exposed to  $\text{N}_2\text{H}_4/\text{H}_2$  rather than to  $\text{N}_2\text{H}_4/\text{He}$ , the general appearance of the absorption spectrum is the same. But the absolute intensities of the bands at 1499  $\text{cm}^{-1}$  and 1469  $\text{cm}^{-1}$  are reduced considerably, whereas those of the other bands are of comparable magnitude or somewhat larger (Table 6).

#### IV DISCUSSION

Earlier studies<sup>4</sup> with Shell-405 catalyst indicated that an adsorbate remained on the catalyst surface following exposure to pulses of hydrazine. The surface-adsorbed species were chemically identified and their binding energies to the catalyst surface deduced by temperature-programmed desorption (TPD).<sup>4</sup> One of the most strongly bound species was found to yield gaseous nitrogen,  $N_2(\beta_2)$ , after the  $Ir/Al_2O_3$  catalyst reached a temperature of about 675 K. The studies indicated that the  $N_2(\beta_2)$  could originate from adspecies involving such precursors as  $NH_2$  and  $NH$  formed by rupture of the N-N bond during hydrazine adsorption. Auger electron spectroscopy did indeed show nitrogen adspecies to be present on catalyst samples removed from operational thrusters.<sup>7</sup> The question then arises if the buildup of surface species leads to the gradual decrease in Ir sites active for  $N_2H_4$  decomposition on Shell-405 catalyst. The experimental results from this year's study further substantiate that reaction intermediates are one of the causes of catalyst deactivation in the  $Ir-N_2H_4$  system.

Kinetic measurements at low pressure demonstrate that temperature is important in the product distribution. Below 550 K, hydrazine decomposes to  $N_2$  and  $NH_3$  almost exclusively [Equation (5)], whereas above 600 K, the products of the reaction [Equation (6)] are  $NH_3$ ,  $N_2$ , and  $H_2$ . These data are in good agreement with earlier results<sup>4</sup> on the product distribution as a function of temperature at atmospheric pressure. In this work, however, no  $NH_3$  was detected as a high-temperature product. Probably, under atmospheric pressure conditions the higher collision frequency led to  $NH_3$  decomposition.

Our results and the current data indicate that the mechanism of hydrazine decomposition on Shell-405 is of zero order in  $N_2H_4$  pressure. In addition, both decomposition paths require very low activation energies. Smith and Solomon<sup>8</sup> report a value of nearly zero, compared with our value of  $2.2 \pm 0.3 \text{ kcal mol}^{-1}$  for the high-temperature reaction [Equation (5)]. At high temperatures we have observed that the pre-exponential term (equivalent to reaction probability per collision) varies with the specific catalyst sample. The catalyst sample obtained from Rocket Propulsion Laboratory (RPL) exhibits much higher activity for  $N_2H_4$  decomposition (that is, a higher preexponential factor) than the sample obtained from Rocket Research Corporation (RRC). These results may be related to variations in Ir metal surface area for the two samples. Indeed, measurement of metal dispersion by our CO-O titration technique<sup>9</sup> indicates that the fresh RPL catalyst has a surface area of  $185 \text{ m}^2/\text{g Ir}$  whereas the fresh RRC catalyst has a surface area of  $154 \text{ m}^2/\text{g Ir}$ . However, the observed variation in activity (a factor of 10) is greater than can be accounted for by the difference in metal dispersion (a factor of 1.2). Also, in a study with selected large pellets from the RPL sample, considerably lower activity was observed than for a random sample. More experimentation is needed to determine the reproducibility of catalyst activity for individual pellets.

Results obtained during low pressure poisoning studies demonstrate a delay in appearance of  $N_2H_4$  decomposition products that increases monotonically with exposure. This effect has also been observed qualitatively during high pressure studies and suggests that the increase in time is associated with  $N_2H_4$  diffusion into the interior of the catalyst pellet. The important role of pore diffusion in catalyst deactivation is further suggested by the results obtained in high pressure studies (1 atm), which demonstrated a significant effect of the particle size of the catalyst on its rate of deactivation (Figure 7).

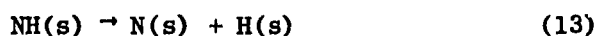
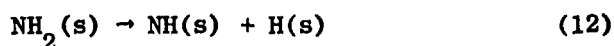
In this work, a powdered sample of Shell-405 having a fraction of its pore structure destroyed during grinding is observed to poison less rapidly than Shell-405 in pelletized form. Additional studies are needed to fully understand the relationship between pore diffusion and catalyst deactivation.

We have observed experimentally that exposure of Shell-405 to carbon monoxide and to toluene reduces catalytic activity for  $N_2H_4$  decomposition. These experiments showed that catalytic activity cannot be completely destroyed by long exposure to these materials. For the CO-exposed catalyst, the original activity can be restored by heating above 900 K. These data are in agreement with earlier TPD studies<sup>8</sup> that showed a desorption maximum for CO near this temperature. Toluene acts as a poison on Shell-405, presumably through carbon deposition, since treatment in  $O_2$  at  $\sim 900$  K is required to restore original activity. These results suggest that hydrocarbon and CO impurities in the  $N_2H_4$  fuel do not completely deactivate the catalyst.

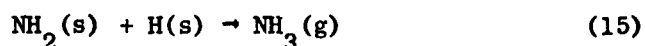
A significant observation made during poisoning studies, at both low and atmospheric pressure, is the effect of temperature on catalyst deactivation. As shown in Figure 5, a maximum in catalyst deactivation is observed near 450 K, close to the temperature found in low pressure studies. The temperature pattern of catalyst poisoning follows closely the rate of desorption of surface-adsorbed hydrogen ( $\alpha$ -hydrogen), an intermediate detected in temperature-programmed desorption studies<sup>4</sup> of the adsorbate retained by the catalyst after exposure to  $N_2H_4$  (Figure 6). Mechanistically, we conclude that because of the rapid depletion of H-atoms by recombination and  $H_2$  desorption at 450 K, the  $NH_2(s)$  surface intermediate formed in  $N_2H_4$  decomposition,



can undergo further dehydrogenation to strongly bound nitrogen adatoms N(s):



rather than ammonia formation by:



Only at temperatures above 450 K the reaction  $2\text{N}(\text{s}) \rightarrow \text{N}_2$  takes place. Based on such a mechanism, one would conclude that in the presence of  $\text{H}_2$  the deactivation process is modified. Such an effect has actually been observed. As shown on Figures 6 and 19, the decline of Shell-405 activity is substantially reduced in the presence of  $\text{H}_2$ . Low-pressure studies indicate that heating a partially deactivated catalyst in  $\text{H}_2$  is effective in restoring a large fraction (~80%) of the initial activity.

Catalyst reactivation by exposure to He at elevated temperature demonstrates that temperatures above 673 K are required to restore the initial activity for hydrazine decomposition (Table 1). Similar results were obtained in low pressure studies. This observation is consistent with the presence of NH adspecies, which desorb<sup>4</sup> with  $\text{N}_2$  and  $\text{H}_2$  as products at temperatures above 673 K.

These kinetic results, in agreement with ir data, suggest that  $\text{NH}_2$  adspecies on the surface of the Ir crystallites are the precursors to catalyst poisoning. Their removal requires reaction with H-adatoms to form  $\text{NH}_3$  or high temperature desorption (> 675 K) with  $\text{N}_2$  and  $\text{H}_2$  as

products. In the latter case, however, the formation of strongly bound N-adatoms may lead to irreversible deactivation of the Ir surface (nitride formation) as observed in catalyst samples removed from thrusters.<sup>6</sup>

## V CONCLUSION

Our results on  $N_2H_4$  decomposition catalyzed by  $Ir/Al_2O_3$  as derived from a combination of experimental techniques (kinetic studies at high and low pressures and infrared measurements) point to the presence of a reaction intermediate, as the surface contaminant likely to be responsible for  $Ir/Al_2O_3$  deactivation. The data obtained from these studies indicate that the temperature region around 440 K is most detrimental to long-term operation of a hydrazine monopropellant fuel thruster because of the maximum rate of  $NH_2$  adspecies buildup on the catalyst observed at this temperature. At somewhat higher temperatures, catalyst activity is less severely affected by this surface species because it undergoes progressive dehydrogenation and eventual desorption as  $N_2$  and  $H_2$ . Based on these results, we would predict that longer catalyst life might be achieved by continuous operation at temperatures above 673 K. However, irreversible processes leading to the formation of a surface metal nitride and sintering of the catalyst may contraindicate long exposures at excessively high temperatures.

## VI REFERENCES

1. R. C. Cosser and F. C. Tompkins, *Trans. Faraday Soc.* 67, 526 (1971).
2. R.C.A. Contaminand and F. C. Tompkins, *Trans. Faraday Soc.* 67, 545 (1971).
3. B. J. Wood and H. Wise, *J. Catalysis* 39, 471 (1975).
4. J. L. Falconer and H. Wise, *J. Catalysis* 43, 220 (1976).
5. D. M. Golden, G. N. Spokes, and S. W. Benson, *Angew. Chemie (Int. Ed.)* 12, 534 (1973).
6. J. A. Groenewegen and W.M.H. Sachtler, *J. Catalysis* 27, 369 (1972).
7. S. W. Benson, J. L. Falconer, D. M. Golden, S. E. Stein, H. Wise and B. J. Wood, SRI Annual Report, July 25, 1975, prepared for AFOSR.
8. Owen T. Smith and Wayne C. Solomon, "Kinetics of Hydrazine Decomposition on Iridium and Alumina Supported Iridium Catalysts," Final Report AFRPL-TR-73-59, August 1973.
9. J. Falconer, P. R. Wentreck, and H. Wise, "Interactions with Adsorbed Species for Surface Area Measurement of Iridium Catalysts," AFOSR Technical Report 1976, *J. Catalysis* (in print).

Table 1

REACTIVATION OF Ir/Al<sub>2</sub>O<sub>3</sub> CATALYST IN  
He AT VARIOUS TEMPERATURES\*

Temperature °K	Fractional N <sub>2</sub> H <sub>4</sub> Conversion (%) <sup>†</sup>
297	0.40 <sup>‡</sup>
472	0.51
573	0.55
673	0.61
724	0.98

\*  $5.5 \times 10^{-3}$  g of Ir/Al<sub>2</sub>O<sub>3</sub> (10 wt%); heating  
time = 20 min.

<sup>†</sup> Measured at 298 K on exposure to pulse of N<sub>2</sub>H<sub>4</sub>  
( $6.3 \times 10^{-6}$  moles).

<sup>‡</sup> After exposure to 16.8 moles N<sub>2</sub>H<sub>4</sub>/g in  
temperature range 371 to 623 K.

Table 2

SUMMARY OF IR SPECTRA OBSERVED ON  
 Ir/Al<sub>2</sub>O<sub>3</sub> and on Al<sub>2</sub>O<sub>3</sub> EXPOSED TO N<sub>2</sub>H<sub>4</sub> or NH<sub>3</sub> \*

Band (cm <sup>-1</sup> )	(Assign)	Ir/Al <sub>2</sub> O <sub>3</sub>		Al <sub>2</sub> O <sub>3</sub>	
		N <sub>2</sub> H <sub>4</sub>	NH <sub>3</sub>	N <sub>2</sub> H <sub>4</sub>	NH <sub>3</sub>
~ 3474	OH	VS, B	m, B	M, B	M, B
~ 3335	N <sub>2</sub> H <sub>4</sub> , NH <sub>3</sub>	VS, B	S, B	S, B	S, B
~ 3177	NH	VS, B	S, B	M, B	M, B
1688	NH <sub>3</sub>	A	W	A	A
1623	OH, N <sub>2</sub> F <sub>4</sub>	M	A	M	A
1603	N <sub>2</sub> H <sub>4</sub>	S	A	M	M
1588	NH <sub>3</sub>	A	M	A	A
1549	NH	A	A	W	A
1499	NH <sub>2</sub>	M	A		
1469	NH <sub>4</sub> <sup>+</sup>	W	M	A	A
1360		A	A	A	W
1261-1271	NH <sub>3</sub>	W	W	W	W

\* N<sub>2</sub>H<sub>4</sub> - NH<sub>3</sub> Exposure = 6.0 x 10<sup>-3</sup> moles at 295 K

VS = very strong

S = strong

M = medium

W = weak

A = absent

B = broad

Table 3

SPECIFIC SURFACE ASSIGNMENTS FOR  
 INFRARED BANDS FOUND ON  $N_2H_4$  - EXPOSED  $Ir/Al_2O_3$

Band ( $cm^{-1}$ )	Assignment/Surface
~ 3474	$OH/Al_2O_3$
1623	$OH/Al_2O_3$
1603	$N_2H_4/Al_2O_3$
1499	$NH_2/Ir$
1469	$NH_4^+/Ir$

Table 4  
 EFFECT OF N<sub>2</sub>H<sub>4</sub> EXPOSURE ON INFRARED BANDS OBSERVED ON Ir/Al<sub>2</sub>O<sub>3</sub>

N <sub>2</sub> H <sub>4</sub> Exp. mol x 10 <sup>3</sup> Band (cm <sup>-1</sup> )	Absorbance (log I <sub>0</sub> /I)						% Band Change
	0.8	6.2	7.4	10.4	34.2		
~ 3474	0.47	0.35	0.39	0.29	0.38		-19
~ 3335	0.53	0.57	-	0.60	0.71		+34
~ 3177	0.48	0.50	0.51	0.50	0.63		+31
1623	0.17	0.21	0.22	0.28	0.30		+76
1603	0.12	0.30	0.28	0.38	0.36		+200
1549	-	-	0.09	0.11	0.11		+22
1499	0.09	0.15	0.14	-	0.21		+133
1469	0.09	0.05	0.04	0.05	0.08		-11
1261-1271	0.02	0.05	0.02	0.06	0.03		+50

Table 5

EFFECT OF HEATING IN He\* ON ABSORPTION SPECTRUM OF  
Ir/Al<sub>2</sub>O<sub>3</sub> EXPOSED TO HYDRAZINE†

Band (cm <sup>-1</sup> )	Absorbance (log I <sub>0</sub> /I)				
	Temperature (K)				
	295	373	473	573	725
~ 3474	0.32	~ 0	~ 0	~ 0	~ 0
~ 3335	0.39	~ 0	~ 0	~ 0	~ 0
~ 3177	0.35	~ 0	~ 0	~ 0	~ 0
1623	0.12	0.04	~ 0	~ 0	~ 0
1603	0.21	0.10	0.03	0.03	0.03
1499	0.15	0.12	0.08	0.05	0.04
1469	0.05	0.04	0.03	0.03	0.02
1261-1271	0.05	0.01	0.01	~ 0	~ 0

\* For 15 minutes at He flow rate of 30 cc/min

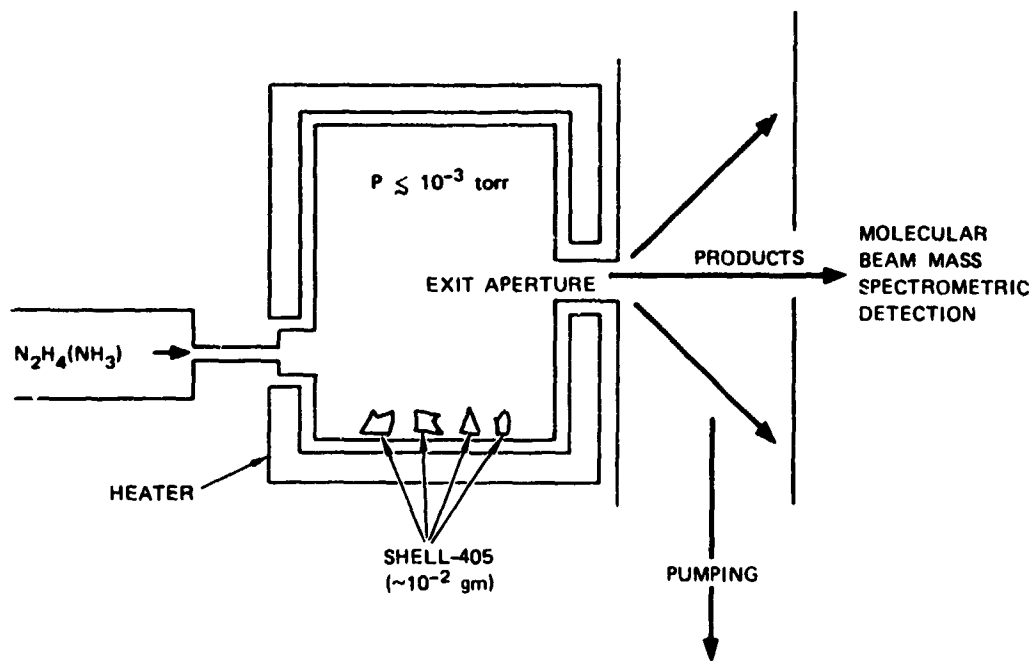
† 6.0 x 10<sup>-3</sup> moles at 295 K

Table 6

EFFECT OF H<sub>2</sub> ON THE INFRARED SPECTRUM OF  
N<sub>2</sub>H<sub>4</sub>-EXPOSED Ir/Al<sub>2</sub>O<sub>3</sub>\*

Band (cm <sup>-1</sup> )	Absorbance (log I <sub>0</sub> /I)	
	N <sub>2</sub> H <sub>4</sub> /He	N <sub>2</sub> H <sub>4</sub> /He/H <sub>2</sub>
~ 3474	0.35	0.36
~ 3335	0.57	0.69
~ 3177	0.50	0.57
1623	0.21	0.24
1602	0.30	0.30
1499	0.15	0.08
1469	0.05	0.01
1261-1271	0.05	0.05

\* Total N<sub>2</sub>H<sub>4</sub> exposure = 6.0 x 10<sup>-3</sup> moles; gas  
composition = 1 vol% N<sub>2</sub>H<sub>4</sub>/43 vol% H<sub>2</sub>/56 vol% He.

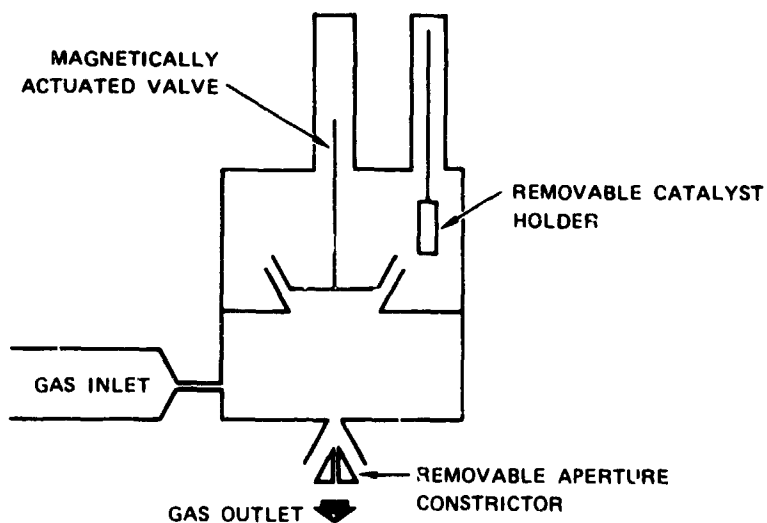


SA-2716-47

$N_2H_4$  FLOW RATE IN =  $N_2H_4$  FLOW RATE OUT +  $N_2H_4$  DECOMPOSITION RATE  
 AT LOW PRESSURE (MEAN FREE PATH > PELLET DIAMETER)

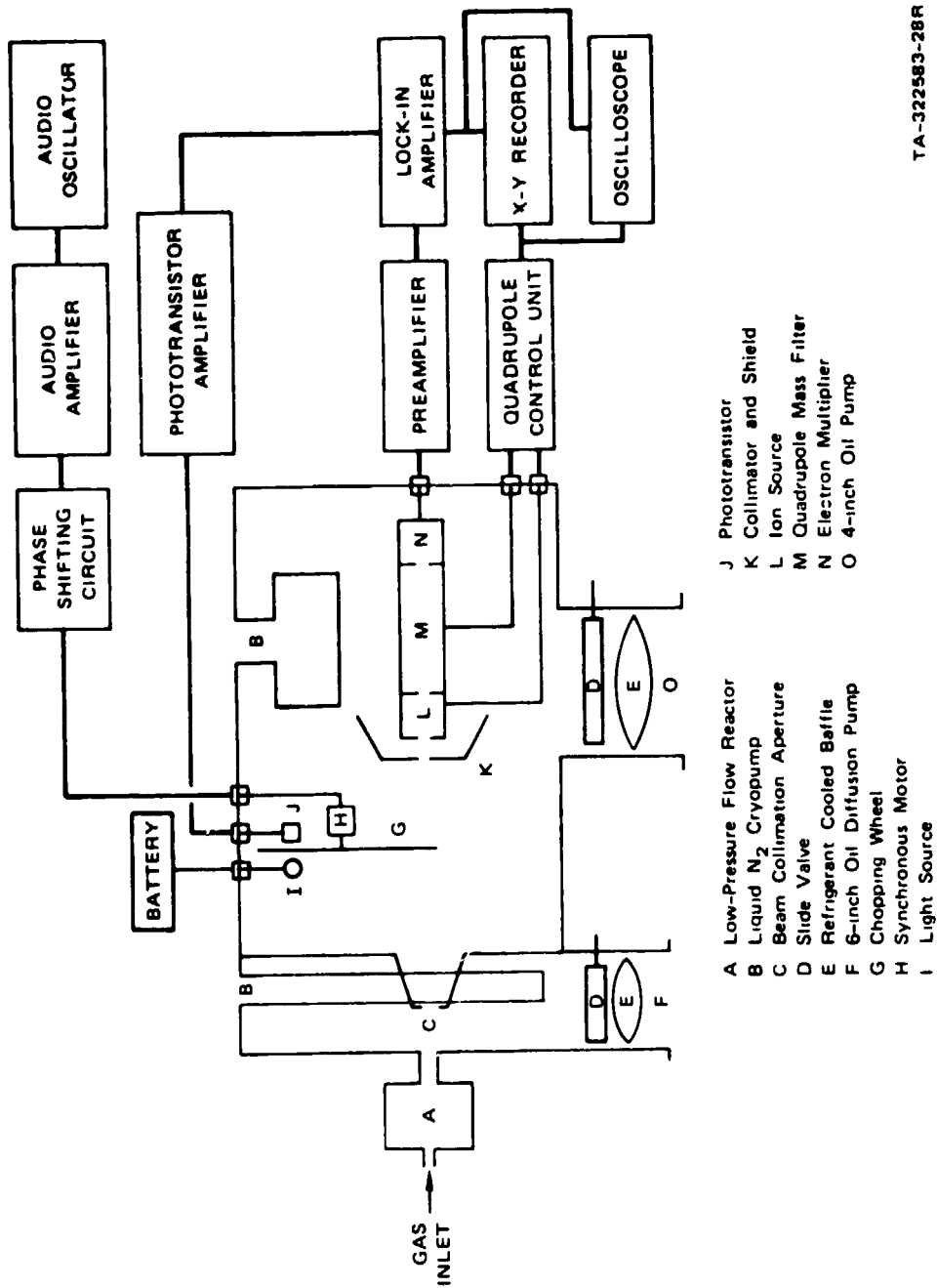
$$\text{REACTION PROBABILITY PER COLLISION WITH CATALYST EXTERIOR} = \frac{\text{EFFECTIVE EXIT AREA}}{\text{EFFECTIVE EXTERNAL CATALYST AREA}} \left( \frac{\text{FRACTION DECOMPOSED}}{\text{FRACTION REMAINING}} \right)$$

FIGURE 1 KNUDSEN FLOW REACTOR (R1) FOR MEASURING RATE OF  $N_2H_4$  DECOMPOSITION ON SHELL-405 CATALYST



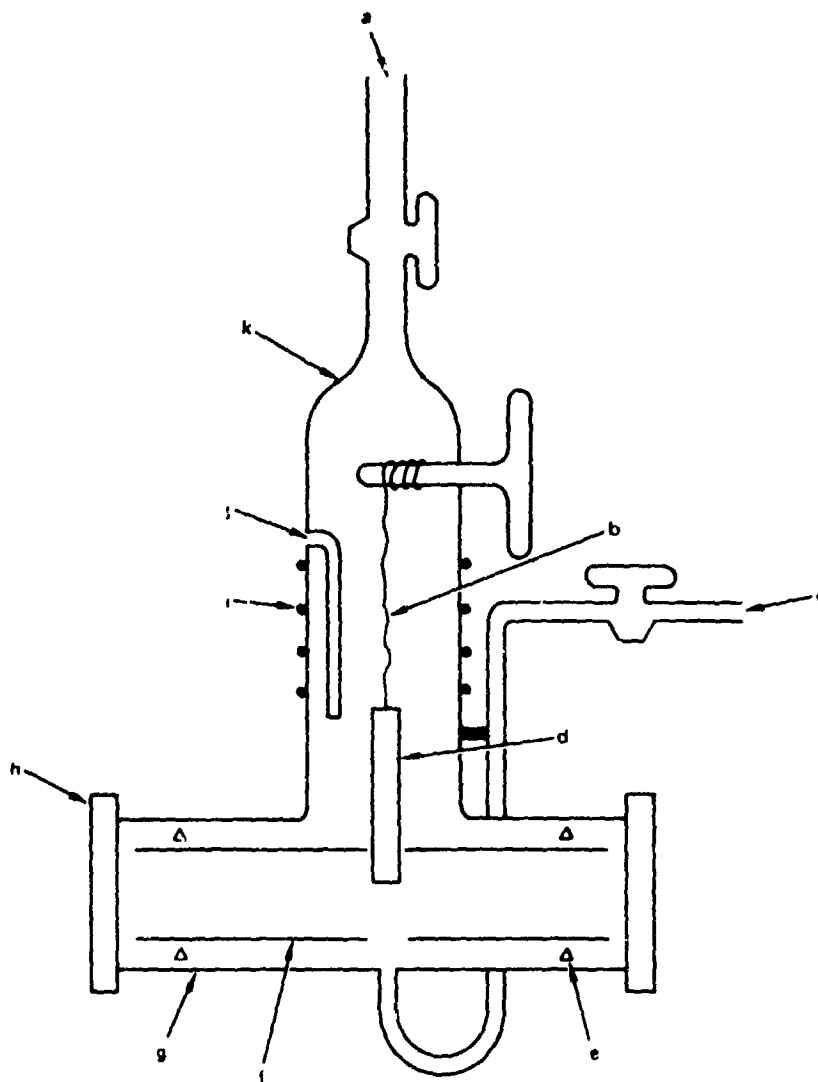
SA-2716-39

FIGURE 2 FUSED SILICA DUAL-CHAMBER LOW PRESSURE FLOW REACTOR (R2)



TA-322583-28R

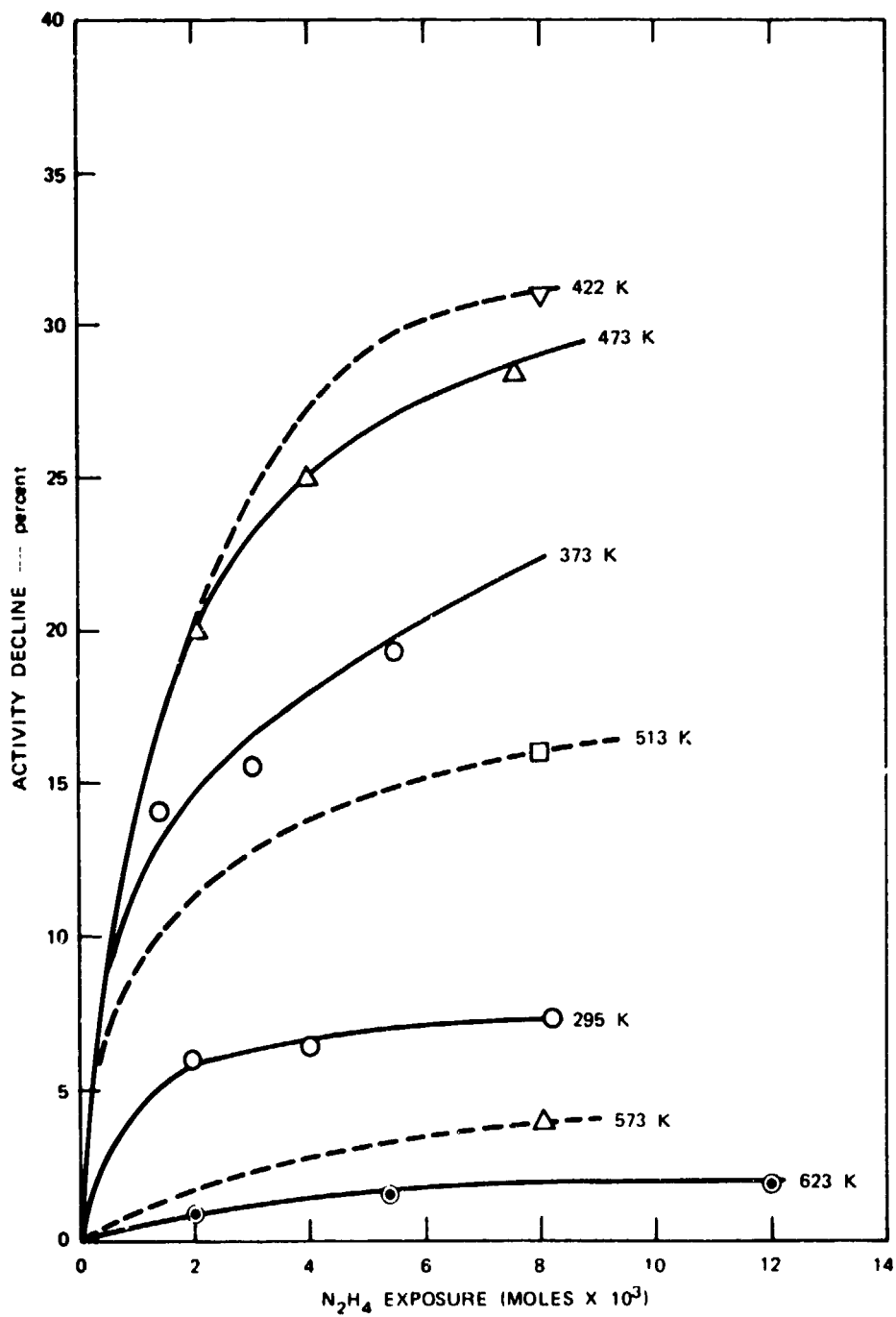
FIGURE 3 SCHEMATIC DIAGRAM OF DIFFERENTIALLY-PUMPED MODULATED-MOLECULAR-BEAM MASS SPECTROMETRIC DETECTION SYSTEM FOR LOW PRESSURE FLOW REACTOR



- (a) Gas Outlet
- (b) Pyrex String
- (c) Gas Inlet
- (d)  $BaF_2$  Crystal 8 x 8 x 25 mm
- (e) Teflon Sleeve
- (f) Sample Holder
- (g) Horizontal Section 70 mm x 25.4 mm
- (h) NaCl Window
- (i) Nichrome Heating Wire
- (j) Thermowell
- (k) Vertical Section 130 mm x 21 mm

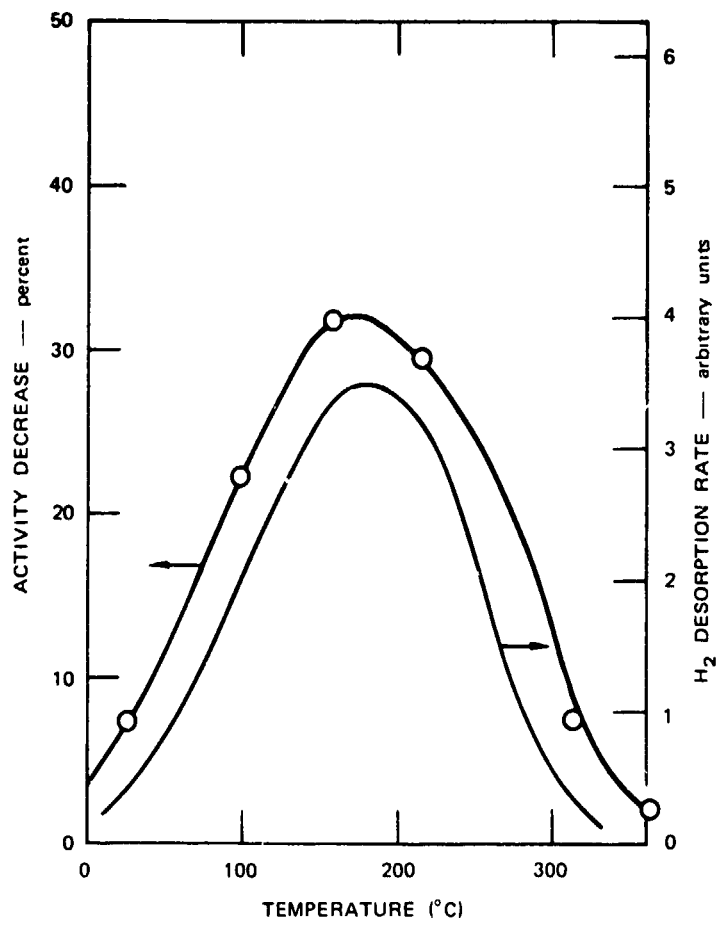
SA-1945-44

FIGURE 4 THE INFRARED CELL



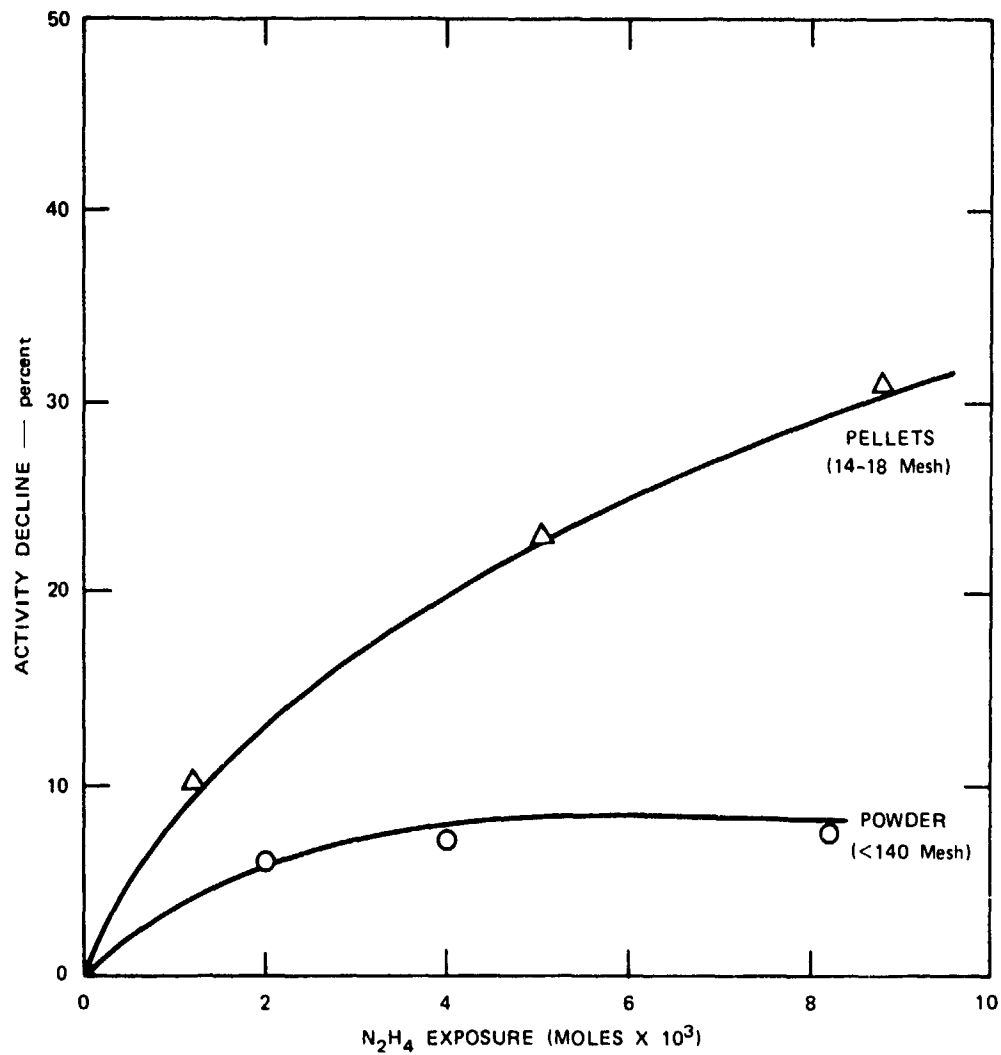
SA-2716 51

FIGURE 5 CATALYST ACTIVITY DECREASE AS A FUNCTION OF TEMPERATURE AND N<sub>2</sub>H<sub>4</sub> EXPOSURE (5.5 X 10<sup>-3</sup>g 10 wt % Ir/Al<sub>2</sub>O<sub>3</sub>)



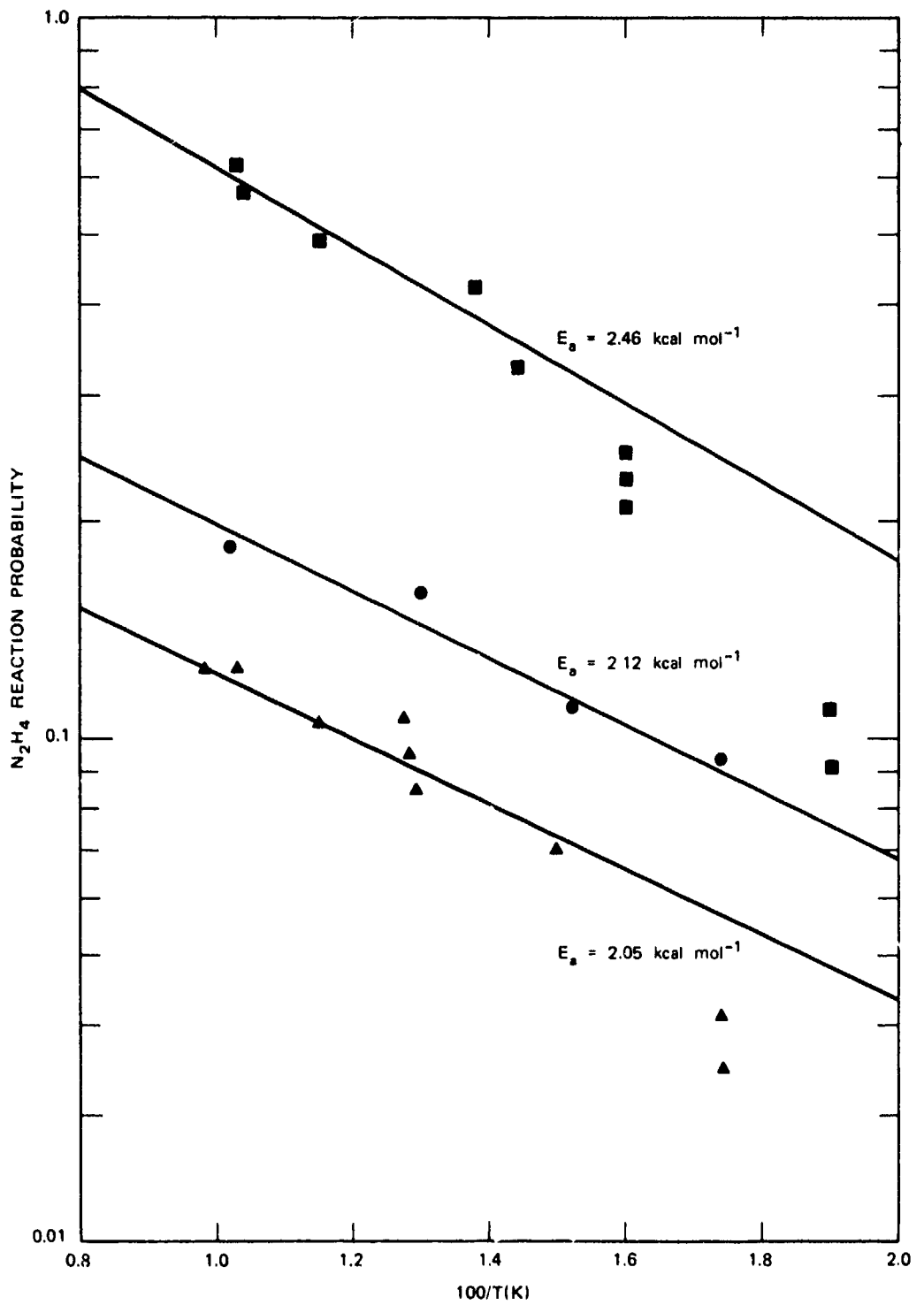
SA-2716-40R

FIGURE 6 CATALYST ACTIVITY DECREASE AFTER EXPOSURE TO  $8.0 \times 10^{-3}$  MOLE  $N_2H_4$  (10 wt % Ir/Al<sub>2</sub>O<sub>3</sub>)



SA-2716-52

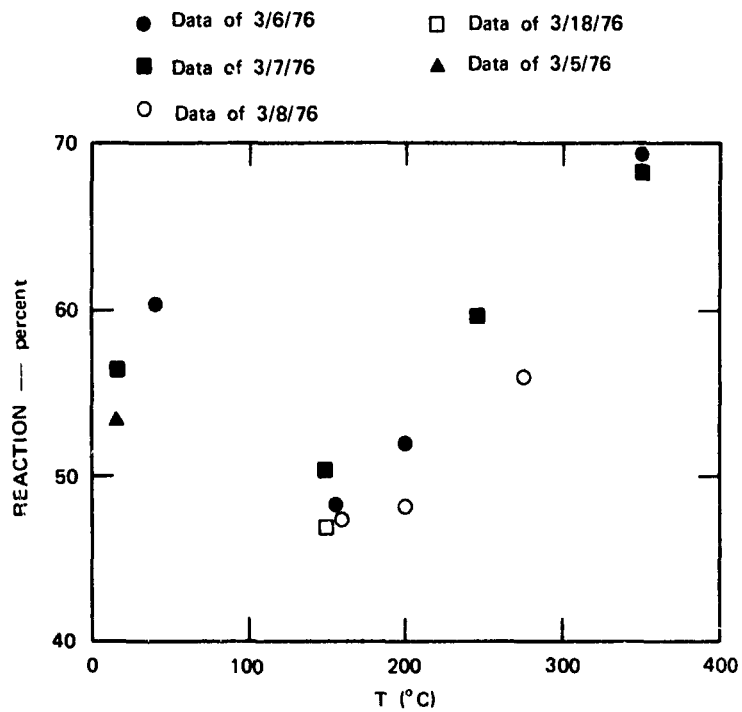
FIGURE 7 EFFECT OF CATALYST PARTICLE SIZE ON ACTIVITY DECLINE AT 298 K (5.5 mg 10 wt % Ir/Al<sub>2</sub>O<sub>3</sub>)



SA-2716-42R

FIGURE 8 ARRHENIUS PLOT OF HIGH-TEMPERATURE  $N_2H_4$  DECOMPOSITION ON SHELL-405

- Five Average Fresh Pellets from RPL
- Two Large Fresh Pellets from RPL
- ▲ Five Average Fresh Pellets from RRC



SA-2716-46R

FIGURE 9 REACTIVITY OF ACTIVATED SHELL-405 FOR  $N_2H_4$  DECOMPOSITION

Catalyst activated by heating to 1000 K under  $H_2$  exposure. Percentage decomposition determined under  $N_2H_4$  flow rate  $\sim 10^{15}$  molec  $sec^{-1}$ .

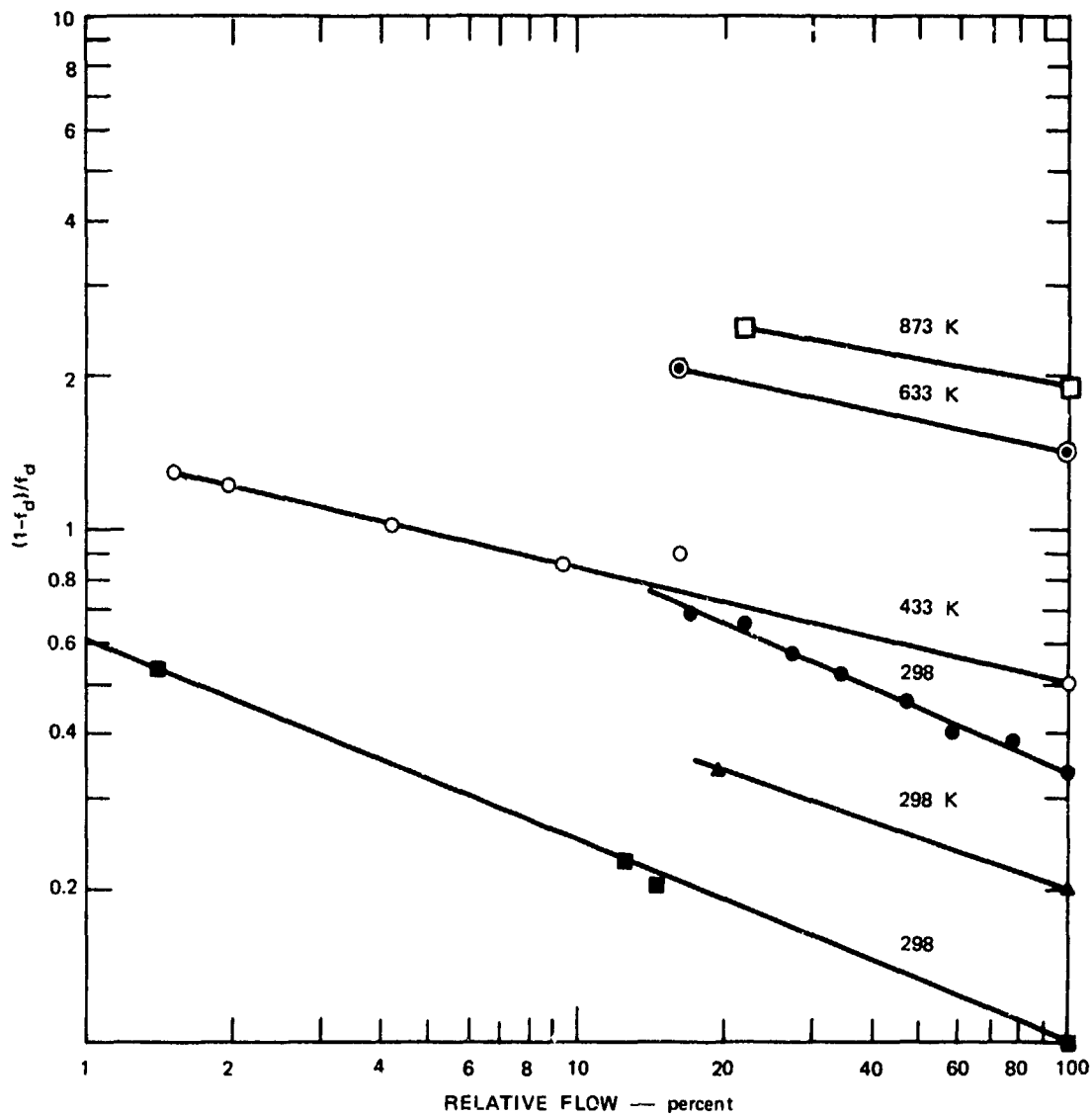
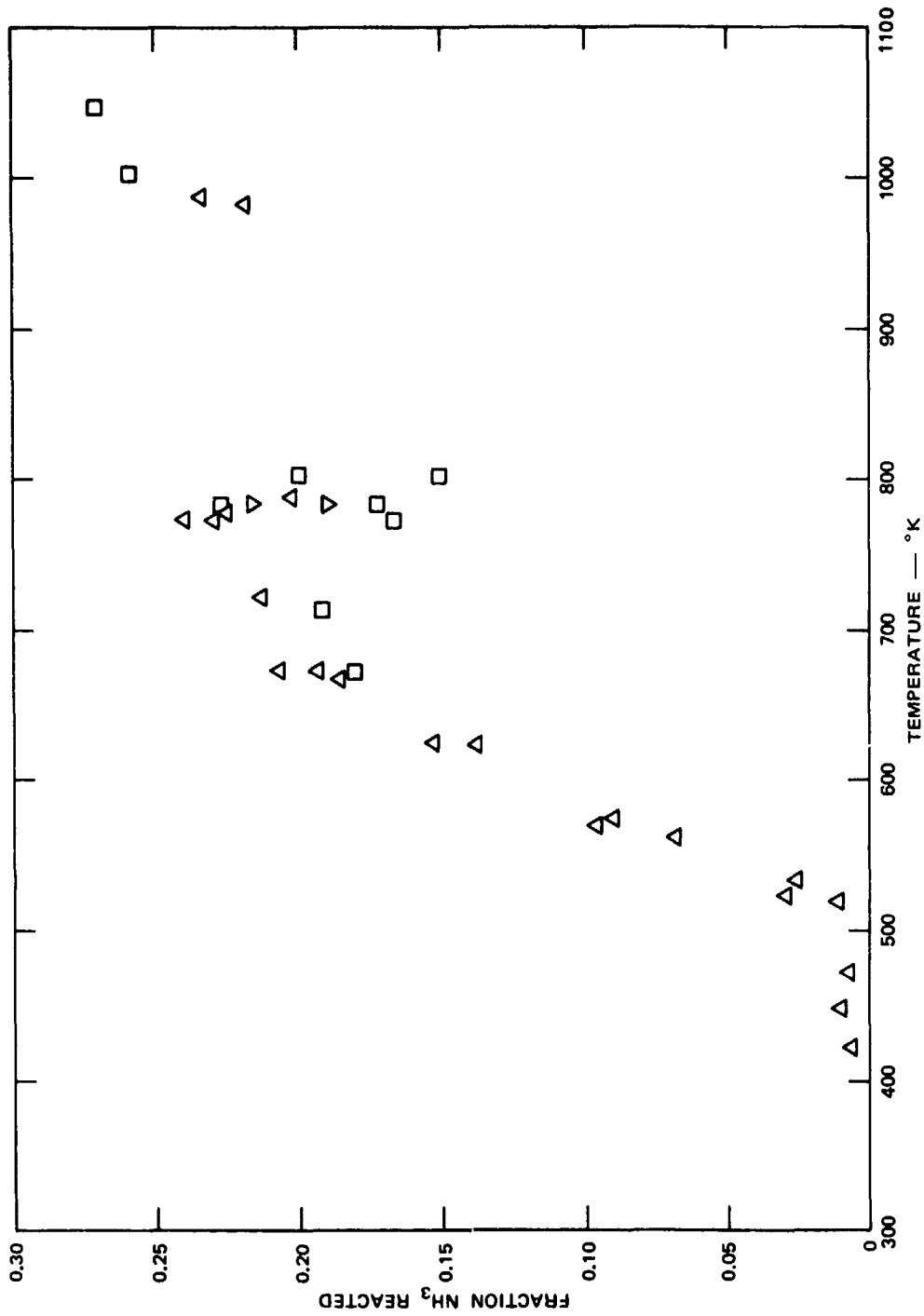


FIGURE 10 MEASURE OF  $N_2H_4$  DECOMPOSITION AS A FUNCTION OF FLOW RATE

- Fresh Catalyst
- ⊙ Fresh Catalyst
- Fresh Catalyst
- ▲ Catalyst Partially Poisoned
- Catalyst Poisoned by Exposure to  $N_2H_4$
- Catalyst Reactivated by Heating to 1000 K with  $H_2$



SA-2716-34

FIGURE 11 DECOMPOSITION OF AMMONIA ON FRESH SHELL-405 (32 wt % Ir)

The average number of collisions of a NH<sub>3</sub> molecule with the external surface of shell-405 before escape is ~30 collisions molec<sup>-1</sup>. Pressure on NH<sub>3</sub> is ~10<sup>-3</sup> torr.

Run No. 1 Δ ; No. 2 ▽ ; No. 3 □ .

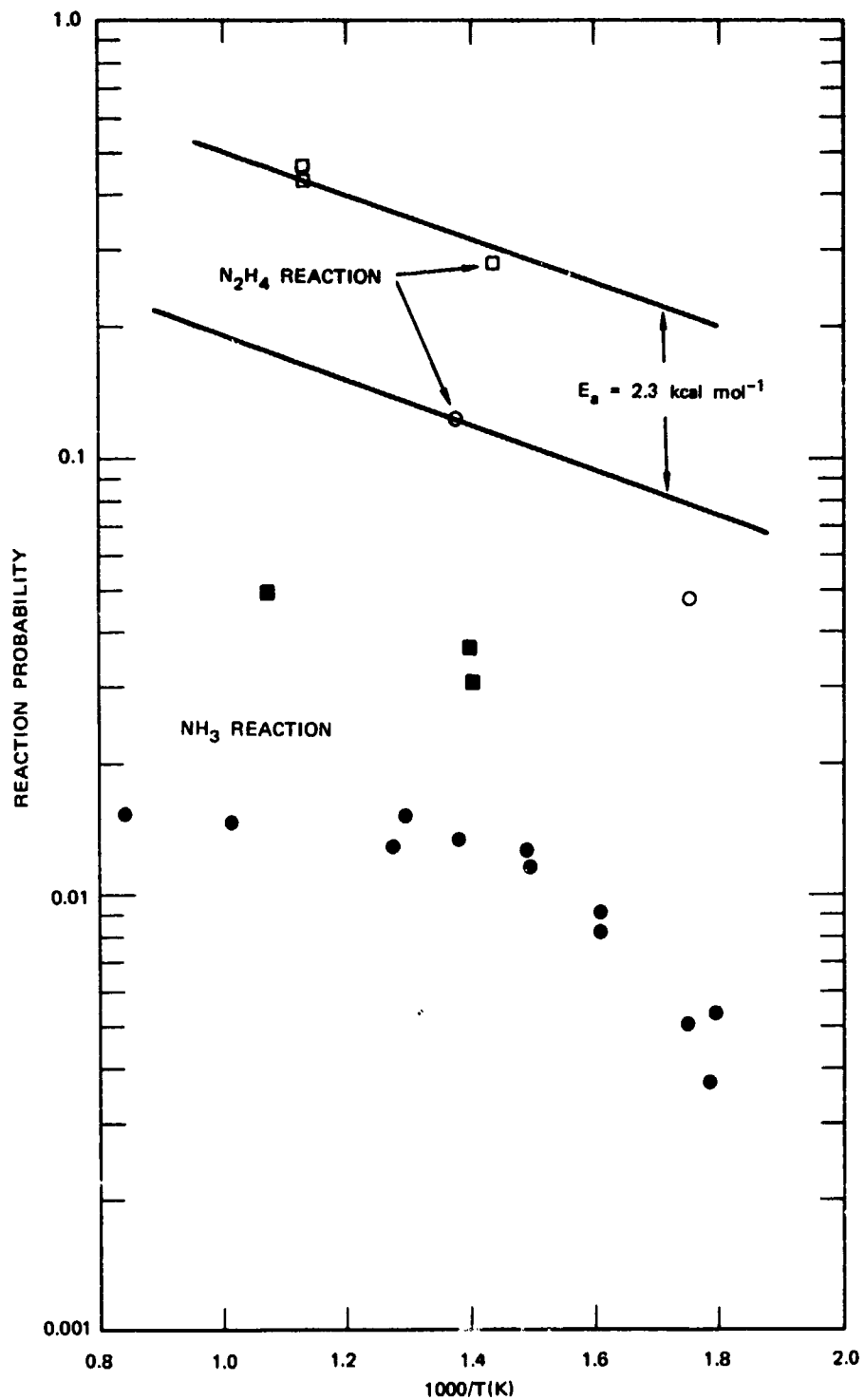


FIGURE 12 COMPARISON OF  $N_2H_4$  AND  $NH_3$  REACTION PROBABILITY ON TWO SAMPLES OF FRESH SHELL-405

Flow  $\sim 2 \times 10^{16}$  molecules  $\text{scc}^{-1}$

- ■  $N_2H_4$  and  $NH_3$ , Respectively, Reaction on Six Pellets from RRC
- ●  $N_2H_4$  and  $NH_3$ , Respectively, Reaction on Five Pellets from RPL

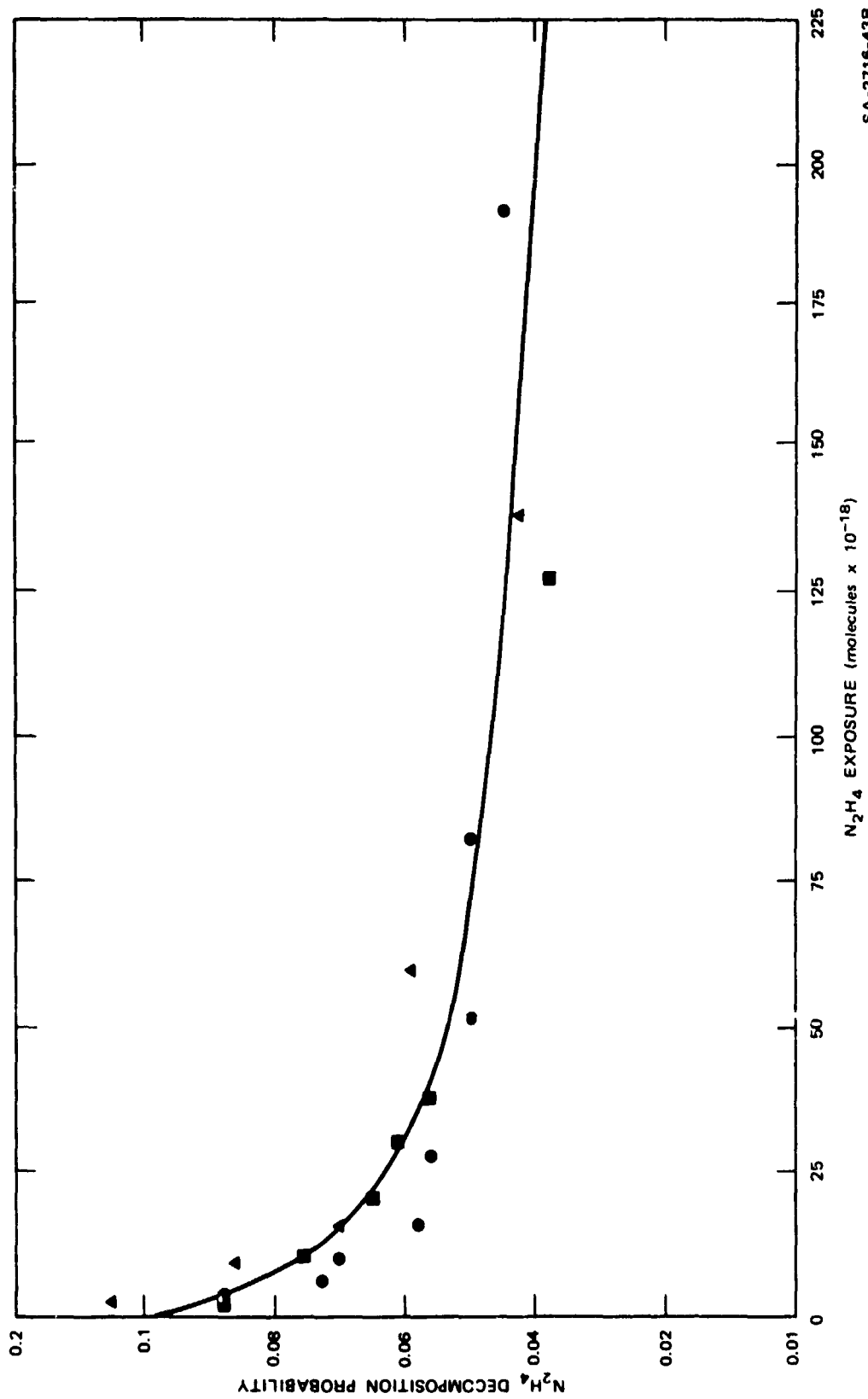


FIGURE 13 REVERSIBLE DEACTIVATION OF SHELL-405 CATALYST RESULTING FROM N<sub>2</sub>H<sub>4</sub> EXPOSURE AT 298 K

Catalyst was activated before N<sub>2</sub>H<sub>4</sub> exposure by heating in vacuum to 1000 K  
 N<sub>2</sub>H<sub>4</sub> flow = 2 × 10<sup>18</sup> molec sec<sup>-1</sup>

▲ Five Pellets from RPL. Determinations Separated by 4 Days  
 ● Five Different Pellets from RPL

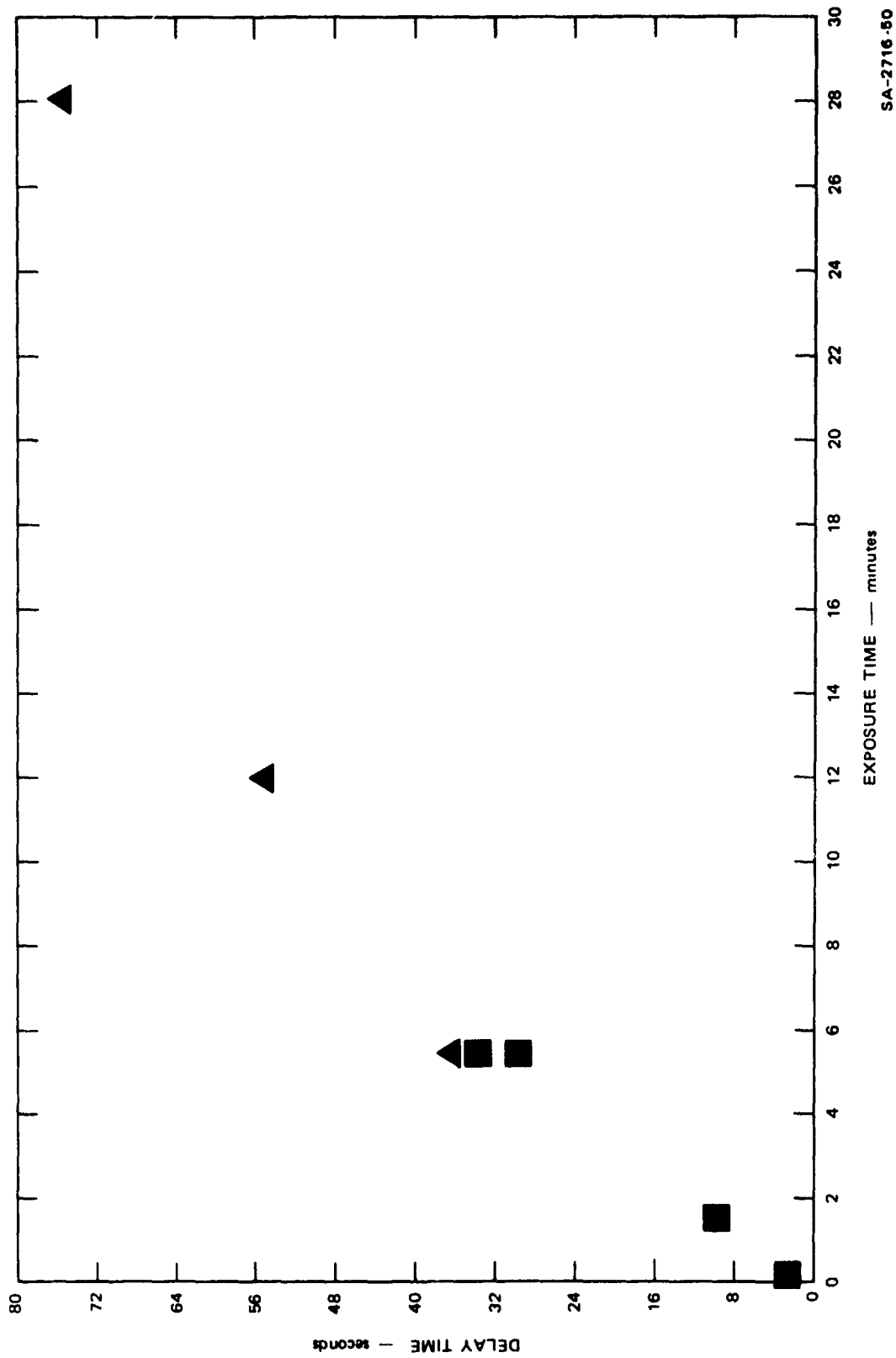
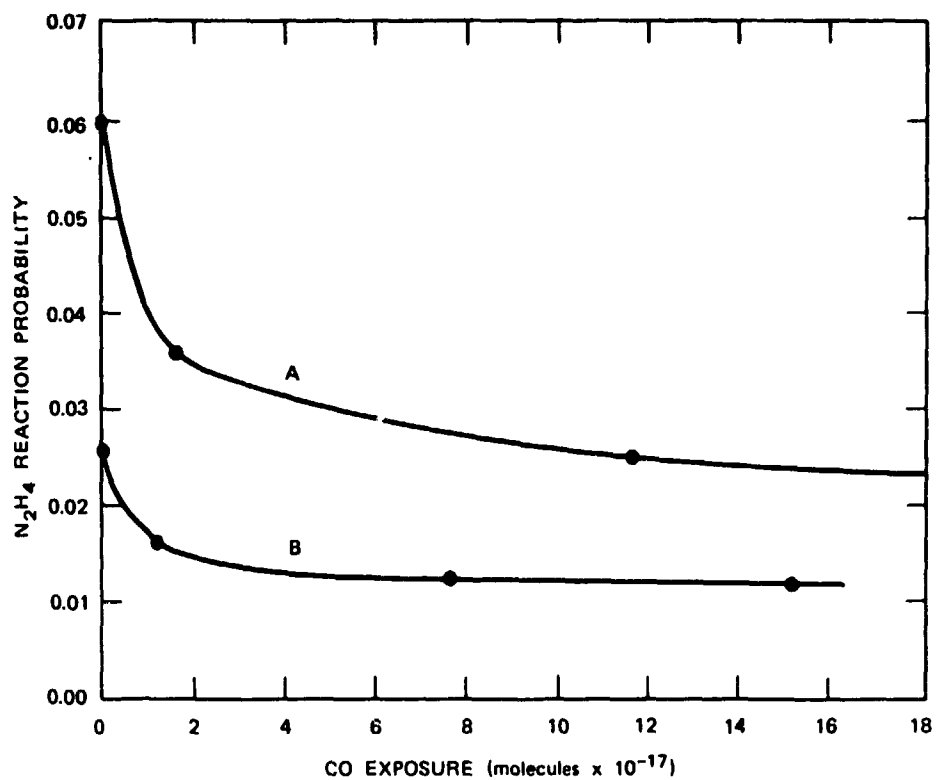


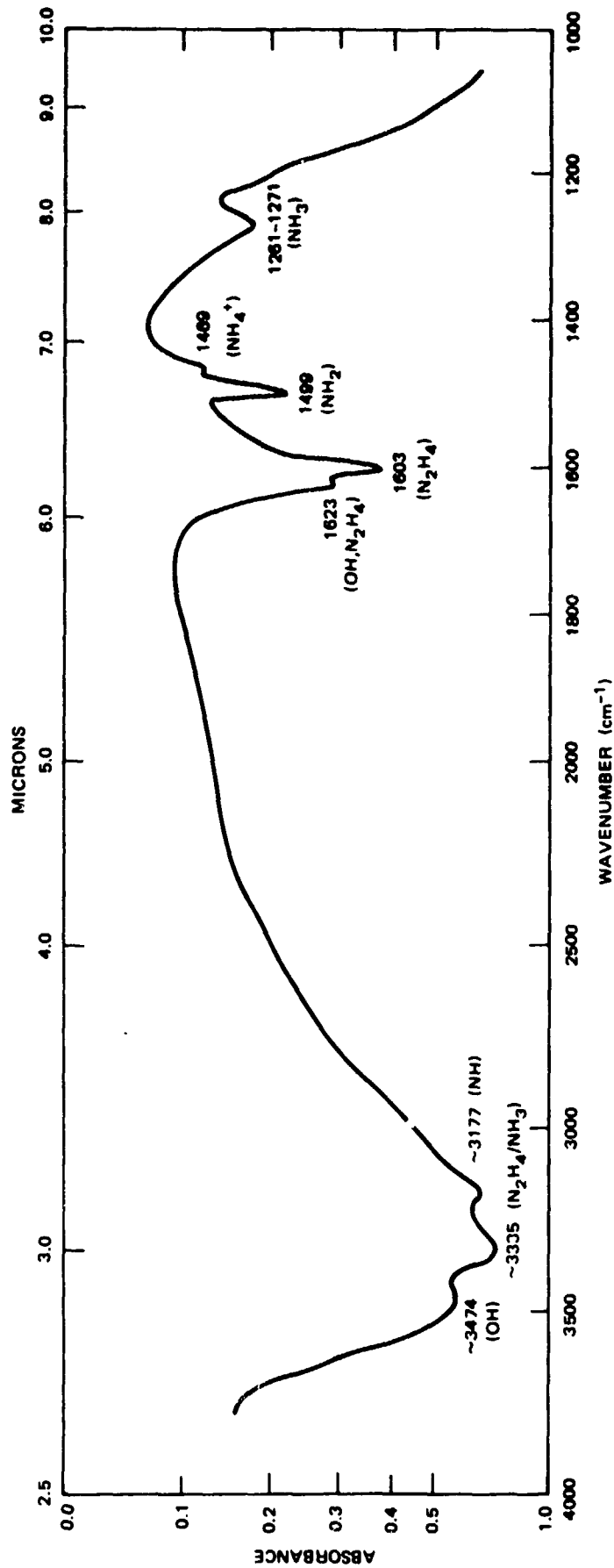
FIGURE 14 EFFECT ON  $N_2H_4$  EXPOSURE ON DELAY TIME  
 Delay times determined under  $N_2H_4$  flow rate  $\sim 10^{15}$  molecules  $sec^{-1}$   
 Exposure flow  $\sim 10^{17}$  molecules  $sec^{-1}$

- Catalyst Activated by Heating to 1000 K Under  $H_2$  Exposure
- ▲ Catalyst Partially Poisoned



SA-2716-44R

FIGURE 15 CATALYST DEACTIVATION BY CO EXPOSURE AT 298 K  
 A - Catalyst Activated Before CO Exposure by Heating to 1000 K  
 B - Catalyst First Heated to 1000 K and Exposed to  $N_2H_4$  at 298 K



SA-2716-63

FIGURE 16 INFRARED SPECTRUM OF Ir/Al<sub>2</sub>O<sub>3</sub> EXPOSED TO N<sub>2</sub>H<sub>4</sub> (6.0 X 10<sup>-3</sup> MOLES)

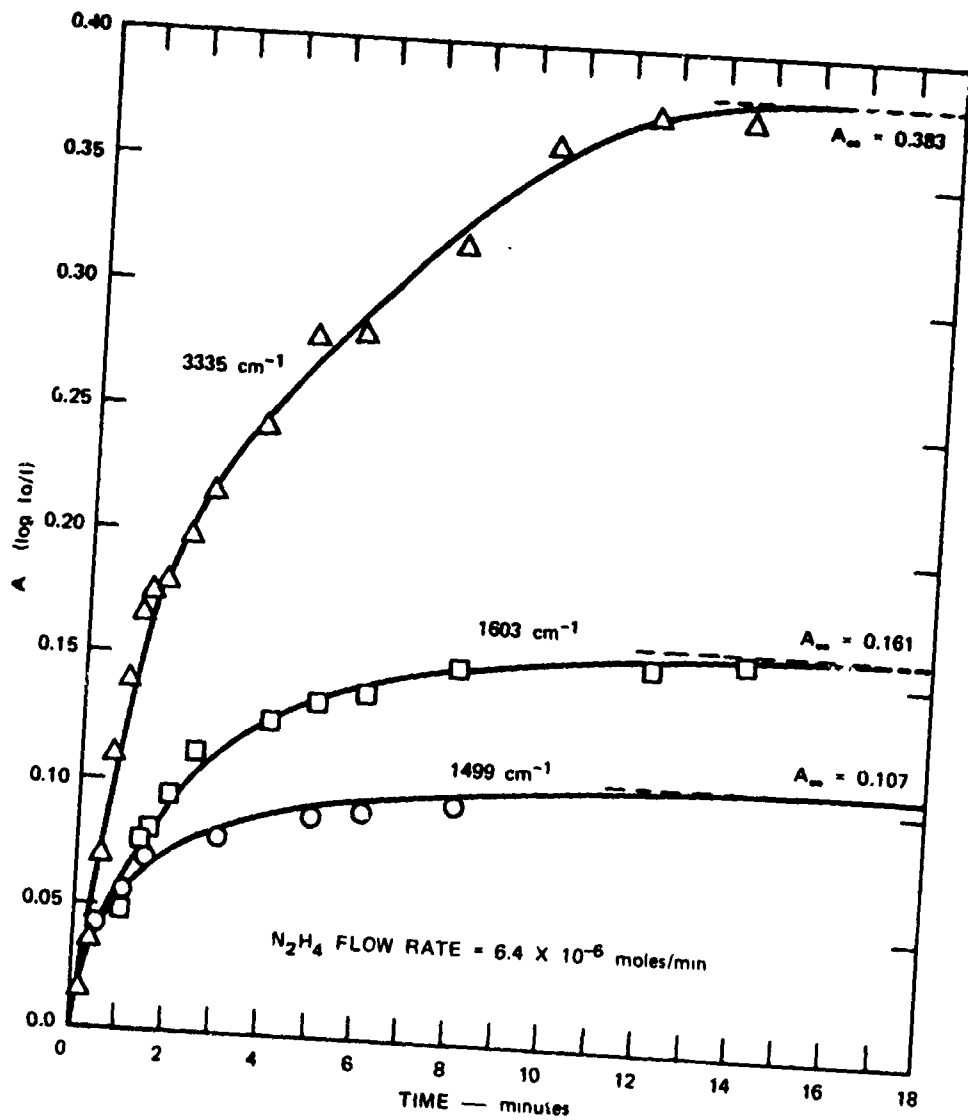
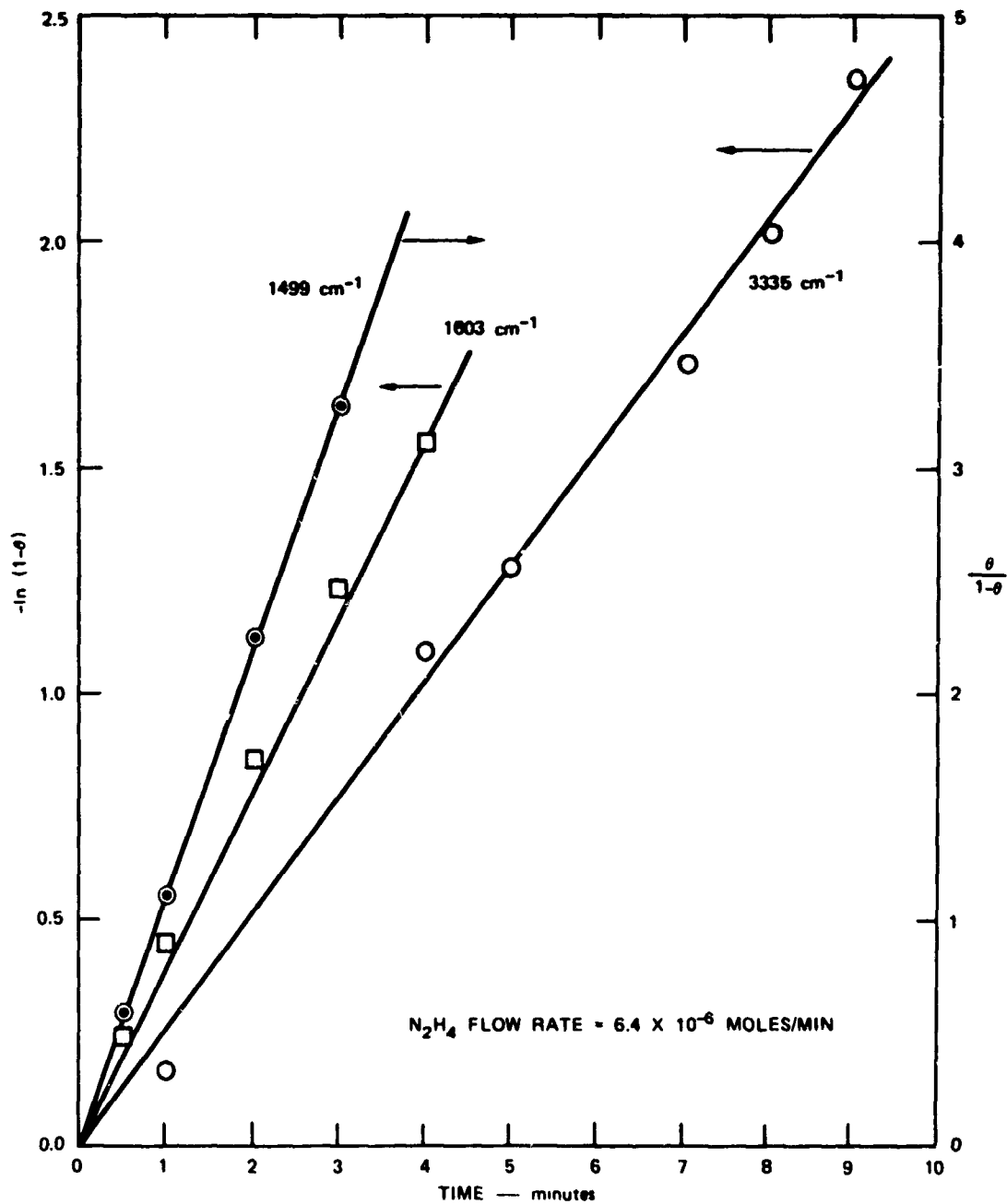
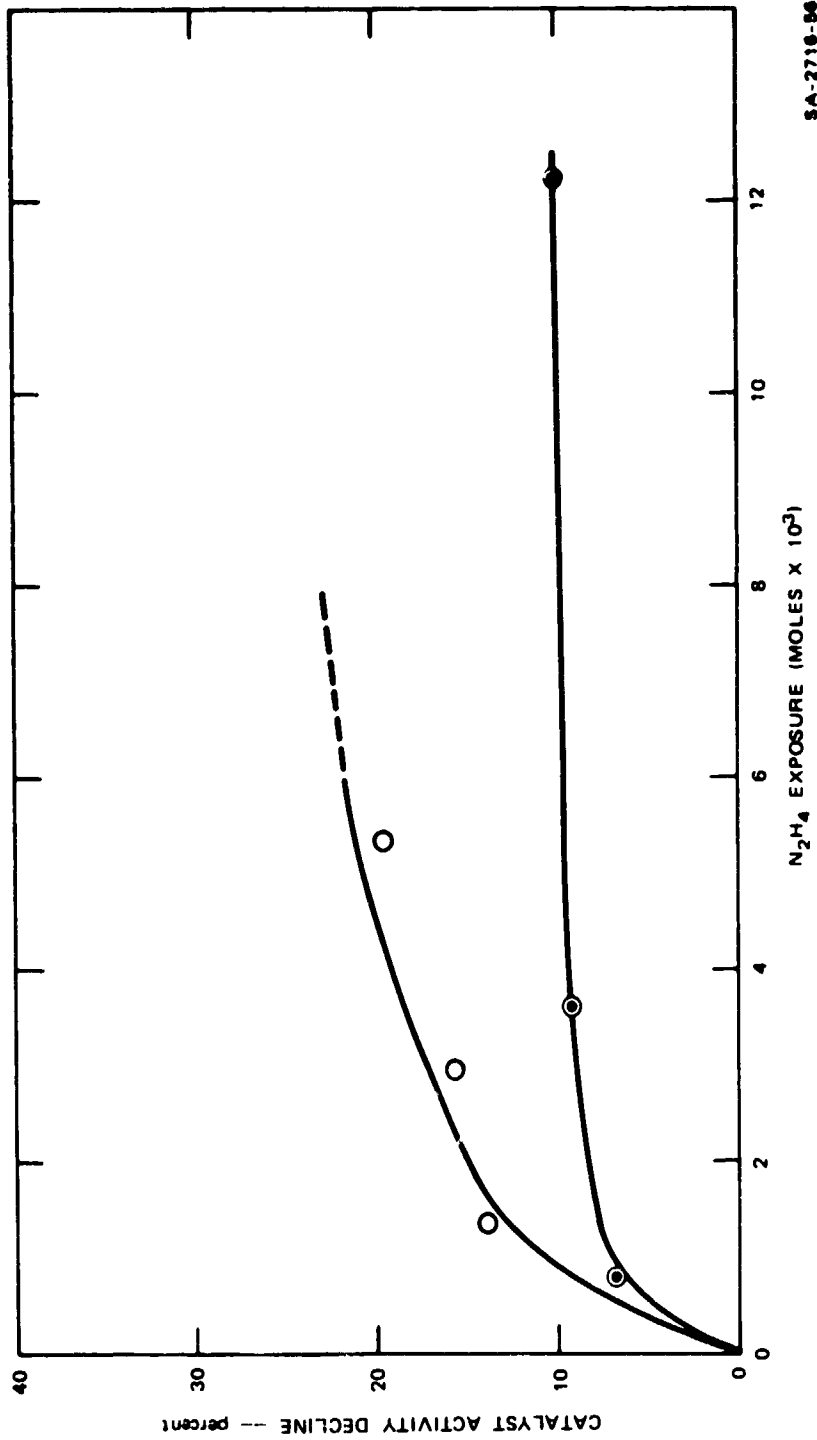


FIGURE 17 FORMATION OF 3335, 1603, AND 1499  $cm^{-1}$  BANDS ON Ir/Al<sub>2</sub>O<sub>3</sub> AS A FUNCTION OF N<sub>2</sub>H<sub>4</sub> EXPOSURE



SA-2716-55

FIGURE 18 KINETIC ANALYSIS OF FORMATION RATES OF 3335, 1603, AND 1499  $cm^{-1}$  BANDS ON  $Ir/Al_2O_3$  AS A FUNCTION OF  $N_2H_4$  EXPOSURE



SA-2716-66

FIGURE 19 EFFECT OF  $H_2$  ON CATALYST DEACTIVATION DURING  $N_2H_4$  EXPOSURE AT 373 K

- 1 vol %  $N_2H_4/43$  vol %  $H_2/56$  vol % He
- 1 vol %  $N_2H_4/99$  vol % He